

# VisionCreator: A Native Visual-Generation Agentic Model with Understanding, Thinking, Planning and Creation

Jinxiang Lai<sup>2\*</sup>, Zexin Lu<sup>1\*</sup>, Jiajun He<sup>1</sup>, Rongwei Quan<sup>1</sup>, Wenzhe Zhao<sup>1</sup>, Qinyu Yang<sup>1</sup>, Qi Chen<sup>1</sup>, Qin Lin<sup>1†</sup>, Chuyue Li<sup>1</sup>, Tao Gao<sup>1</sup>, Yuhao Shan<sup>1</sup>, Shuai Shao<sup>1</sup>, Song Guo<sup>2§</sup>, Qinglin Lu<sup>1†</sup>

<sup>1</sup>Tencent Hunyuan, <sup>2</sup>Hong Kong University of Science and Technology

\*Equal contribution, <sup>§</sup>Corresponding Author, <sup>†</sup>Project lead



## Abstract

Visual content creation tasks demand a nuanced understanding of design conventions and creative workflows—capabilities challenging for general models, while workflow-based agents lack specialized knowledge for autonomous creative planning. To overcome these challenges, we propose **VisionCreator**, a native visual-generation agentic model that unifies Understanding, Thinking, Planning, and Creation (UTPC) capabilities within an end-to-end learnable framework. Our work introduces four key contributions: (i) **VisGenData-4k** and its construction methodology using metacognition-based **VisionAgent** to generate high-quality creation trajectories with explicit UTPC structures; (ii) The VisionCreator agentic model, optimized through **Progressive Specialization Training (PST)** and **Virtual Reinforcement Learning (VRL)** within a high-fidelity simulated environment, enabling stable and efficient acquisition of UTPC capabilities for complex creation tasks; (iii) **VisGenBench**, a comprehensive benchmark featuring 1.2k test samples across diverse scenarios for standardized evaluation of multi-step visual creation capabilities; (iv) Remarkably, our VisionCreator-8B/32B models demonstrate superior performance over larger closed-source models across multiple evaluation dimensions. Overall, this work provides a foundation for future research in visual-generation agentic systems.

## 1 Introduction

AI-assisted visual content creation has revolutionized workflows from professional design to social media. The field has evolved from single-image generation (Ho et al., 2020; Ramesh et al., 2022; Labs, 2024; Saharia et al., 2022; Lin et al., 2024) to complex multi-modal synthesis (Wu et al., 2025; Xiao et al., 2025; Xu et al., 2025a; Xue et al., 2025; Guo et al., 2025), demanding systems that can understand creative intent, plan multi-step operations, and autonomously execute intricate workflows. As shown in Fig.2, current approaches to autonomous visual creation can be categorized into three main paradigms, each with distinct limitations: (a) *General-purpose Unified Multimodal Models (UMM)* Deng et al. (2025); Li et al. (2025a); Lai et al. (2024); Cui et al. (2025) leverage large-scale pre-training to achieve impressive visual understanding, but lack the domain-specific knowledge required for autonomous creative planning and struggle to decompose complex objectives without extensive prompt engineering. (b) *Workflow-specific Agent* Wu et al. (2025); Xiao et al. (2025); Xu et al. (2025a) employ predefined pipelines for specific domains like movie generation or story creation, but their rigid architectures cannot adapt to diverse creative tasks or handle unexpected outcomes during execution. (c) *Workflow-guided Agent* Xue et al. (2025); Guo et al. (2025) orchestrate external tools through carefully designed prompts and coordination logic, leveraging general language models to interpret requests and sequence operations. However, this approach faces several limitations: (i) Reliance on prompt engineering rather than learned domain knowledge, limiting creative understanding; (ii) Explicitly programmed coordination logic that restricts adaptability to diverse tasks; and (iii) Inability to be jointly optimized end-to-end for creative task performance.

To overcome these limitations, we propose **VisionCreator**, a *native* visual-generation agentic model that unifies Understanding, Thinking, Planning, and Creation (UTPC) capabilities in an end-to-end learnable framework, as shown in Fig.2 (d). Unlike existing approaches that rely

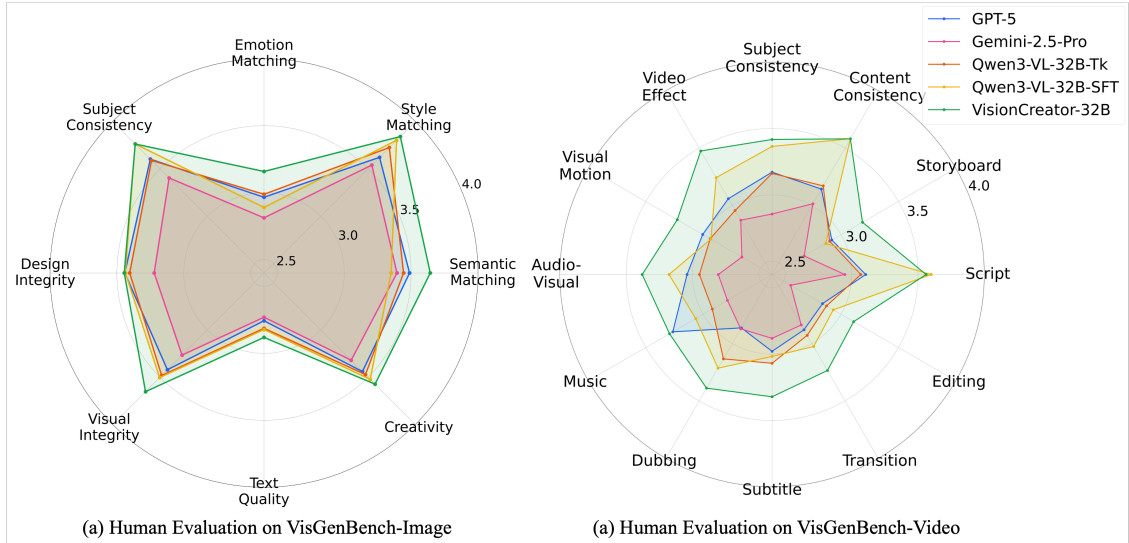


Figure 1: Human Evaluation results on VisGenBench-Image and VisGenBench-Video.

on predefined workflows or external template workflows, our native architecture intrinsically integrates the capabilities of *Understanding* design conventions and user intent, *Thinking* through complex creative constraints, *Planning* multi-step execution trajectories, and *Creation* of high-quality and diverse visual creation tasks. However, realizing this new paradigm faces several critical challenges:

① **Data Bottleneck:** Currently, no comprehensive datasets exist for training agents to perform visual content creation through tool invocation. The lack of high-quality trajectories prevents supervised learning of the UTPC capabilities.

② **Task Complexity:** How to develop models that can handle the full spectrum of visual creation challenges, which encompass (i) Diverse task types, (ii) Varying difficulty levels from basic generation to advanced composition, and (iii) Complex creation tasks requiring 20+ execution steps? Existing approaches face significant limitations: specialized systems excel in narrow domains but fail to generalize across diverse tasks, while general models lack the depth for sophisticated creative reasoning and struggle with long-horizon consistency and adaptive strategy adjustment.

③ **Training Difficulty:** How to establish an effective and efficient training paradigm for such a native agent? The conventional SFT+RL framework faces significant obstacles: (i) SFT phase struggles to balance general capability preservation with domain-specific specialization, often leading to catastrophic forgetting or insufficient expertise; (ii) Direct online RL training with real tools incurs prohibitive costs and instability due to expensive API invocation and limited concurrency. Furthermore, designing accurate reward signals for multi-step creative trajectories is particularly challenging, as imperfect reward functions are highly vulnerable to reward hacking.

To address these challenges, we propose:

(i) **VisGenData-4k with UTPC Structure:** We design a metacognition-based *VisionAgent* to generate a comprehensive dataset following the UTPC structure, featuring diverse visual creation tasks across multiple difficulty levels. Through rigorous human quality inspection, we meticulously filter and retain only the highest-quality data samples. The resulting VisGenData-4k provides diverse and high-quality execution trajectories that explicitly capture *Understanding* of design conventions, *Thinking* through creative constraints, *Planning* of multi-step trajectories, and *Creation* of visual content, offering rich supervision signals for complex creative workflows.

(ii) **Progressive Specialization Training (PST):** We introduce a novel Progressive Specialization Training methodology that cultivates UTPC capabilities through two-stage optimization. PST effectively addresses the generalization-specialization trade-off by first establishing robust *Understanding* and *Thinking* capacities through general foundation learning, followed by targeted domain specialization to enhance *Planning* and *Creation* expertise. This progressive strategy not only prevents catastrophic forgetting of general abilities but also efficiently identifies optimal data composition for stagewise specialization, enabling the model to develop comprehensive UTPC

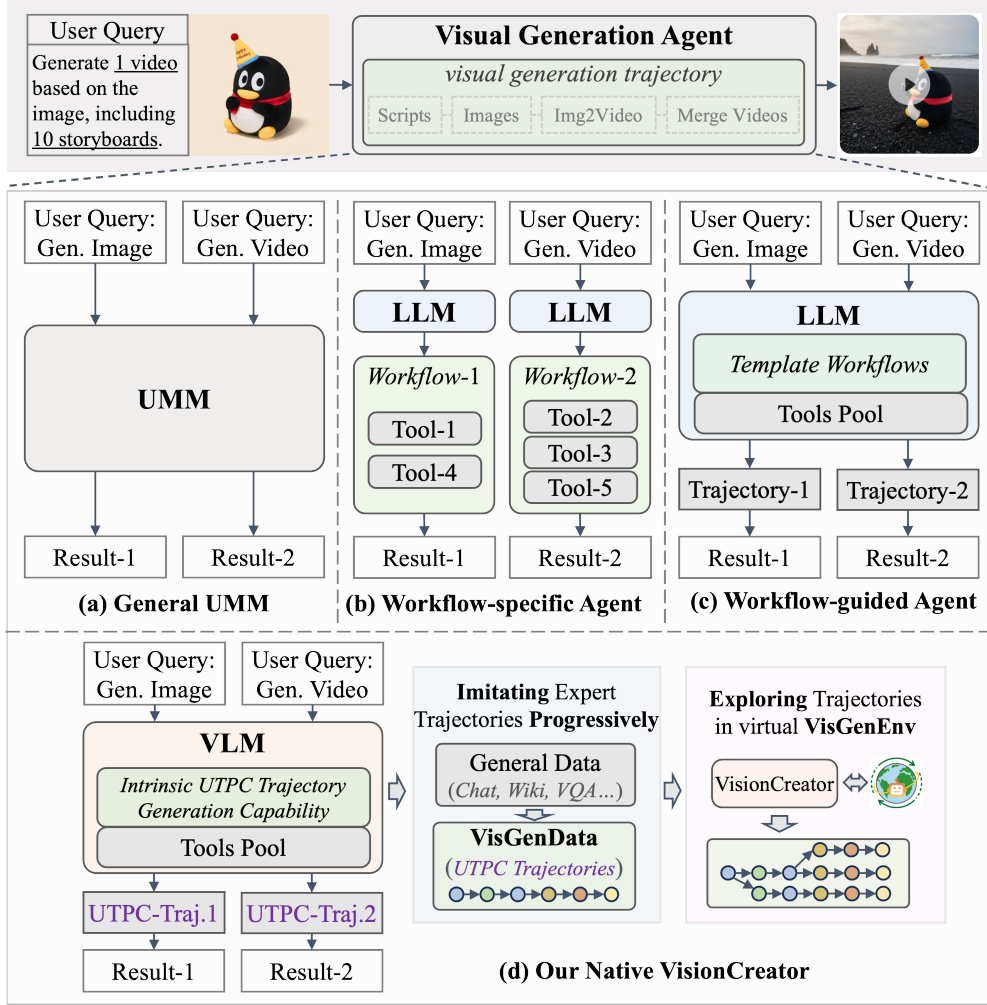


Figure 2: Framework comparisons. (a) UMM. (b) Workflow-specific Agent. (c) Workflow-guided Agent. (d) Our Native VisionCreator.

capacities while maintaining strong cross-domain reasoning abilities.

(iii) **Virtual VisGenEnv Construction:** We construct VisGenEnv, a virtual environment for VRL. It features 36 tools with high-fidelity simulation of their behaviors. Multimodal outputs are simulated by returning random samples from a media database, providing correct physical attributes. This design enables effective learning of workflow planning through accurate tool behavior simulation.

(iv) **Virtual Reinforcement Learning (VRL) with LtrReward:** We develop an innovative *Virtual Reinforcement Learning (VRL)* paradigm that conducts the entire reinforcement learning using *Long Trajectory Reasoning Reward (LtrReward)* within the high-fidelity *VisGenEnv*. This approach bypasses the prohibitive cost of thousands of GPUs by leveraging simulated tool-call behaviors and functional logic, enabling stable and scalable learning of high-quality planning and action trajectories. Moreover, we provide a theoretical analysis that establishes formal guarantees on sim-to-real transfer and real-world performance improvement.

Finally, we introduce **VisGenBench**, a comprehensive benchmark designed for evaluating *visual generation agentic models* that operate through multi-step tool invocation to accomplish complex image and video creation tasks. Our benchmark encompasses: (i) *Comprehensive Test Suite* - featuring 1.2k test samples including 400 image-generation tasks and 800 video-generation tasks; (ii) *Diverse Applications* - spanning 10 evaluation dimensions across 35+ real-world scenarios; (iii) *Standardized Protocol* - ensuring reproducible evaluation through structured scoring rubrics.

Overall, our contributions are: (i) The VisionCreator, a novel native visual-generation agentic model that unifies UTPC capabilities in an end-to-end learnable framework; (ii) VisGenData-4k and its

construction framework using metacognition-based VisionAgent to generate high-quality creation trajectories with UTPC structures; (iii) A progressive training methodology combining Progressive Specialization Training (PST) and Virtual Reinforcement Learning (VRL) with LtrReward, enabling stable and efficient learning of complex creation trajectories entirely within a virtual environment VisGenEnv; (iv) VisGenBench benchmark with 1.2k test samples across diverse scenarios for standardized evaluation of multi-step visual creation capabilities.

## 2 Related Works

### 2.1 Image Generation

Current image generation models primarily fall into two categories: Autoregressive (Chen et al., 2020; Fan et al., 2024; Han et al., 2024; Tian et al., 2024; Sun et al., 2024; Pang et al., 2024) models and Diffusion (Ho et al., 2020; Ramesh et al., 2022; Labs, 2024; Saharia et al., 2022; Lin et al., 2024) models. While these models provide powerful single-step image generation capabilities, they primarily focus on the *Creation* aspect of visual content generation. Our VisionCreator builds upon these fundamental generation technologies but extends them by integrating comprehensive *Understanding*, *Thinking*, and *Planning* capabilities. This allows our agent to not only generate individual images but also reason about complex creative requirements and plan multi-step visual creation workflows that leverage these underlying generation models as tools.

### 2.2 Video Generation

Video generation methods build on image models by adding time-based processing. Approaches like Make-A-Video (Singer et al., 2022) and SVD (Blattmann et al., 2023) extend image generation to video, while newer architectures like DiT (Peebles & Xie, 2023) and MMDiT (Esser et al., 2024) in models such as CogvideoX (Yang et al., 2024) show progress in handling longer videos. These video generation tools are important for our agent’s creation ability, but they work separately. Our VisionCreator connects these tools through planning and reasoning to handle complete creation tasks.

### 2.3 Visual Generation Agents

Current approaches to autonomous visual creation include three main agent paradigms: (i) Workflow-specific Agents (e.g., MovieAgent (Wu et al., 2025), Captain Cinema (Xiao et al., 2025), MM-StoryAgent (Xu et al., 2025a)) employ predefined pipelines for specialized domains but lack adaptability to diverse creative tasks. (ii) ComfyUI Workflow Generation methods (e.g., ComfyAgent (Xue et al., 2025), ComfyMind (Guo et al., 2025), ComfyUI-R1 Xu et al. (2025b), ComfyGPT Huang et al. (2025)) specialize in generating ComfyUI-format workflows, which limits their visual creation capability in general API scenarios. (iii) Workflow-guided Agents (Xue et al., 2025; Guo et al., 2025) orchestrate external tools through prompt engineering but face limitations in creative understanding depth and end-to-end optimization. These limitations motivate our native visual-generation agent that intrinsically integrates UTPC capabilities in an end-to-end learnable framework.

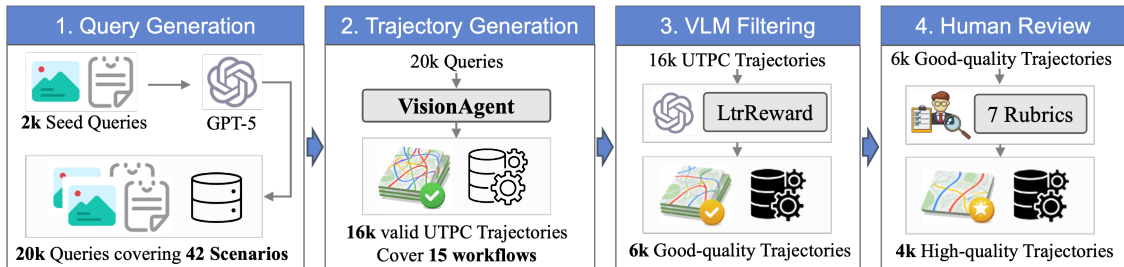


Figure 3: VisGenData-4k construction pipeline.

### 3 VisGenData-4k with UTPC Structure

To tackle the data bottleneck in training visual creation agents, we design VisionAgent, a dataset generation framework based on a Metacognition paradigm. To construct a high-quality VisGenData dataset, VisionAgent employs commercial proprietary models (such as GPT-5, GPT-4o, Veo3, Sora2, etc) for multimodal data generation, and we further filter low-quality trajectories with algorithms and human experts. As shown in Fig. 3, the construction pipeline is as follows: (i) VisionAgent first generates 16k trajectories from 20k queries covering 42 scenarios. (ii) With the rigorous LtrReward and VLM-Grader methods, we remove 10k low-quality trajectories and obtain 6k candidate trajectories. (iii) These subsequently undergo a manual review by human experts, where 2k undesired trajectories are filtered out, resulting in high-quality 4k trajectories.

#### 3.1 VisionAgent for Dataset Construction

As shown in Fig. 4, our VisionAgent generates high-quality execution trajectories that capture the complete reasoning process for complex visual creation tasks. VisionAgent with metacognition achieves a 72% task success rate, representing a 30% improvement over the baseline method that relies solely on thinking.

**Dual-Agent Architecture.** Our framework employs a dual-agent architecture that separates task understanding from execution reasoning: (1) **TaskAgent**: Serves as the task classifier and router. It analyzes user inputs and performs fine-grained task classification across the 21 distinct task types, then selects appropriate predefined workflow templates and tools pool for specific task categories. (2) **MetaAgent**: Functions as the core reasoning engine with metacognitive capabilities. It receives both the selected workflow and tools pool as inputs, then executes structured reasoning through four standardized reasoning types defined in metacognition.

**Metacognitive Reasoning Process.** The metacognition defines four reasoning types: the `<think>` phase maintains situational awareness and todo-list through continuous state evaluation; the `<plan>` phase constructs executable task sequences by decomposing objectives and dependencies; the `<tool.call>` phase invokes appropriate tools based on plan blueprints and analytical reasoning; and the `<answer>` phase verifies goal completion, forming a closed-loop execution process. This Metacognitive reasoning process guides the MetaAgent to generate the UTPC trajectory.

**Reference Workflow Integration.** We incorporate 15 predefined workflow templates as best-practice guides, ensuring planning remains flexible yet stays on track. These workflows provide domain-specific execution patterns for various visual creation tasks, representing 15 distinct application scenarios from storyboards to animated short films.

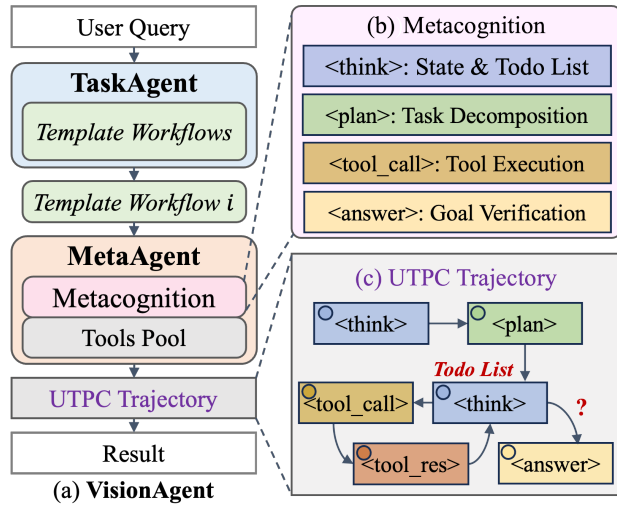


Figure 4: VisionAgent framework for dataset generation.

It receives both the selected workflow and tools pool as inputs, then executes structured reasoning through four standardized reasoning types defined in metacognition.

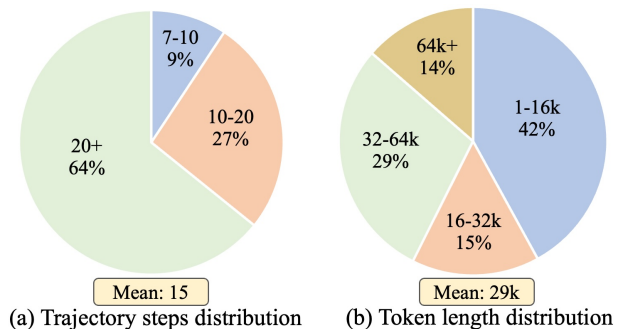


Figure 5: VisGenData-4k dataset statistics.

---

## 3.2 Dataset Composition and Statistics

Fig.5 shows the statistics of our VisGenData-4k, which exhibits the following key features: (1) **Diverse Task Types**: Encompassing 21 distinct task types (including storyboards, marketing posters, product marketing videos, animated short films, etc), this diversity is crucial for training agents to handle a broad range of real-world creative demands, significantly enhancing their adaptability and practical applicability. (2) **Complex Trajectory Structure**: With a mean of 15 steps and 64% of trajectories exceeding 20 steps, this complexity is crucial for training agents to decompose and plan long-horizon tasks, fostering robust problem-solving capabilities in visual creation. (3) **Rich Contextual Information**: The substantial token length (mean: 29k, 43% over 32k) equips agents with the ability to process and utilize extensive contextual cues, significantly enhancing their capacity for detailed and context-aware generation.

## 4 Agentic Post-Training

### 4.1 Agentic Framework

As shown in Fig. 6, VisionCreator is formulated as a unified agent that integrates *Understanding, Thinking, Planning, and Creation* (UTPC) capabilities to accomplish complex visual generation tasks. Formally, we model the agent as a policy  $\pi_\theta$  operating over long-horizon multimodal trajectories:  $\tau = (o_0, a_0, o_1, a_1, \dots, o_T)$ , where  $o_t$  denotes multimodal observations (textual instructions, intermediate tool feedback, and virtual visual states), and  $a_t$  denotes agent actions including reasoning tokens, planning steps, and tool invocations. The training process follows a two-stage agentic post-training paradigm: (1) **Progressive Specialization Training (PST)**, which initializes a strong policy prior via supervised learning over expert UTPC trajectories. (2) **Virtual Reinforcement Learning (VRL)**, which further optimizes long-horizon planning and tool-use strategies through large-scale exploration in a simulated environment.

### 4.2 Progressive Specialization Training

The goal of Progressive Specialization Training (PST) is to learn an initial policy  $\pi_{\theta_0}$  that simultaneously preserves *general reasoning competence* while acquiring *domain-specific visual creation ability*, thereby enabling a functional visual content creation agent rather than a narrowly tuned generator. Let the supervised dataset be  $\mathcal{D} = \mathcal{D}_{\text{gen}} \cup \mathcal{D}_{\text{vis}}$ , where  $\mathcal{D}_{\text{gen}}$  contains large-scale general reasoning and tool-use trajectories, and  $\mathcal{D}_{\text{vis}}$  contains expert-curated visual creation trajectories (VisGenData-4k). Standard supervised fine-tuning (SFT) minimizes

$$\mathcal{L}_{\text{SFT}}(\theta) = \mathbb{E}_{(o,a) \sim \mathcal{D}} [-\log \pi_\theta(a | o)]. \quad (1)$$

However, naive single-stage SFT exhibits two fundamental failure modes. Training only on  $\mathcal{D}_{\text{vis}}$  leads to catastrophic forgetting of general reasoning and planning ability, resulting in nearly zero agent competence; empirically, Tab. 4 shows performance dropping to **0.007**, indicating the model is unable to function as a visual creation agent. Conversely, one-stage mixed SFT on  $\mathcal{D}_{\text{gen}} \cup \mathcal{D}_{\text{vis}}$  avoids catastrophic forgetting but yields *suboptimal specialization*, since the dominance of  $\mathcal{D}_{\text{gen}}$  suppresses learning of visual-creation behaviors and degrades downstream agent performance. These observations reveal a necessary condition for visual agents:

#### General Competence Preservation + Strong Visual Agent Specialization,

which neither naive SFT strategies can satisfy simultaneously.

PST resolves this conflict through a controlled two-stage curriculum that induces a gradual distribution shift. In Stage 1 (general foundation learning),

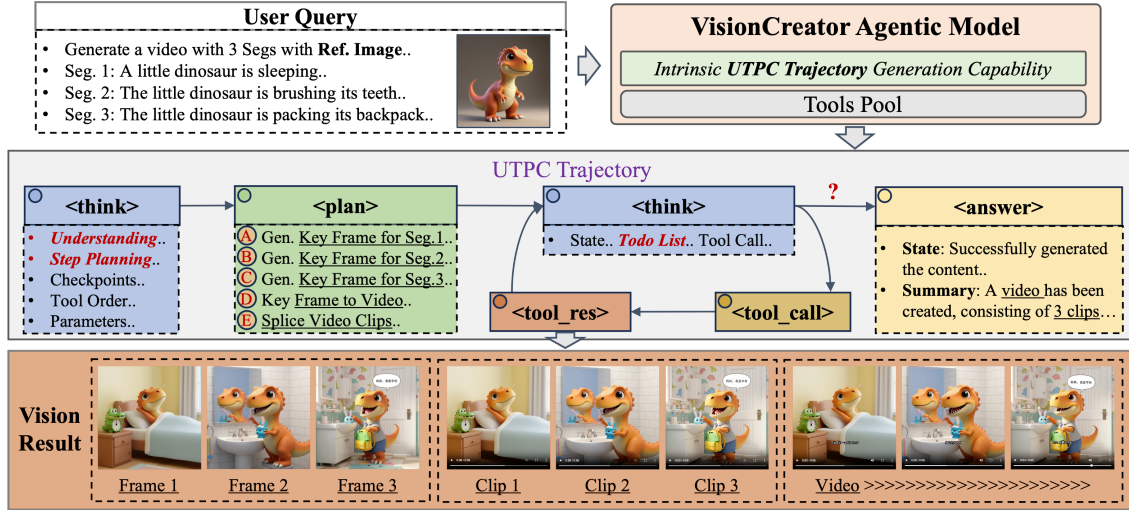
$$\mathcal{D}^{(1)} = \mathcal{D}_{\text{gen}}^{500\text{K}} \cup \lambda \mathcal{D}_{\text{vis}}, \quad (2)$$

establishing robust reasoning, planning, and tool-use capabilities while lightly anchoring the policy to the visual generation agent domain. In Stage 2 (targeted specialization),

$$\mathcal{D}^{(2)} = \mathcal{D}_{\text{gen}}^{200\text{K}} \cup \lambda \mathcal{D}_{\text{vis}}, \quad (3)$$

the increased effective influence of  $\mathcal{D}_{\text{vis}}$  drives specialization toward visual content creation, while continued exposure to  $\mathcal{D}_{\text{gen}}$  prevents catastrophic forgetting. Overall, PST learns a structured initialization

$$\pi_{\theta_0} \approx \arg \min_{\theta} \mathbb{E}_{(o,a) \sim \mathcal{D}^{(1)} \rightarrow \mathcal{D}^{(2)}} [-\log \pi_\theta(a | o)]. \quad (4)$$



(a) Our Native VisionCreator framework

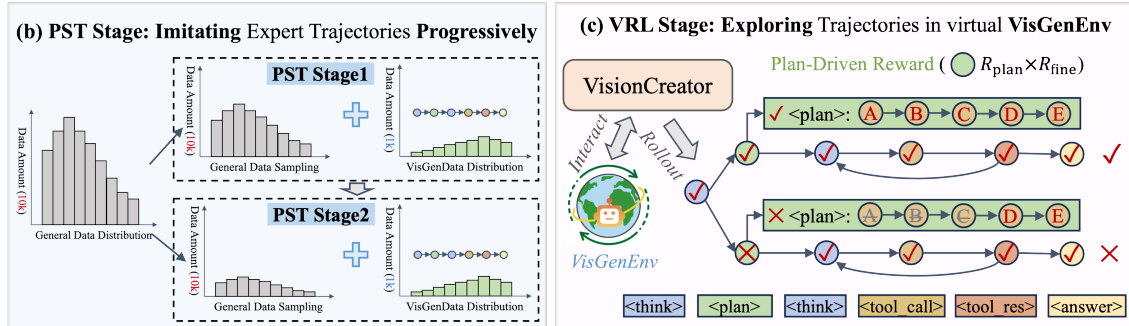


Figure 6: Our Native VisionCreator framework.

which constrains downstream reinforcement learning (RL) to a policy region that already satisfies both general competence and visual specialization. Experimental results further validate the necessity of PST. Compared with one-stage SFT, PST achieves substantially stronger performance on visual creation agent tasks, demonstrating that progressive specialization is essential for learning effective UTPC behaviors. Moreover, PST provides a significantly better initialization for RL: the initial reward score before RL training increases from **0.64** (one-stage SFT) to **0.87** (PST), a gain of **+0.23**. This improved starting point directly translates into optimization efficiency—RL convergence is accelerated by approximately **50%**. These findings confirm that PST not only improves final agent capability, but also fundamentally reduces the difficulty of downstream reinforcement learning.

### 4.3 Virtual Reinforcement Learning

Building upon the robust foundation established by PST, we refine the model’s UTPC capabilities through Virtual Reinforcement Learning (VRL) based on the GRPO algorithm. To enable scalable long-horizon learning without invoking real-world tools, we first construct a high-fidelity virtual environment *VisGenEnv* that simulates the behavior of visual creation tools. Within this environment, LtrReward components are designed to supervise agent trajectories and guide both planning and execution. To understand that policies learned under these rewards transfer effectively to real-world scenarios, we provide a theoretical analysis of VRL. Building upon these insights, we then introduce a plan-driven reward that integrates planning and execution signals to optimize robust long-horizon visual creation performance.

#### 4.3.1 Virtual VisGenEnv Environment

To enable scalable long-horizon learning without invoking real-world tools, we first construct a high-fidelity virtual environment called *VisGenEnv*. This environment serves as a sandbox where the agent can safely explore planning and tool-use strategies, laying the foundation for subsequent

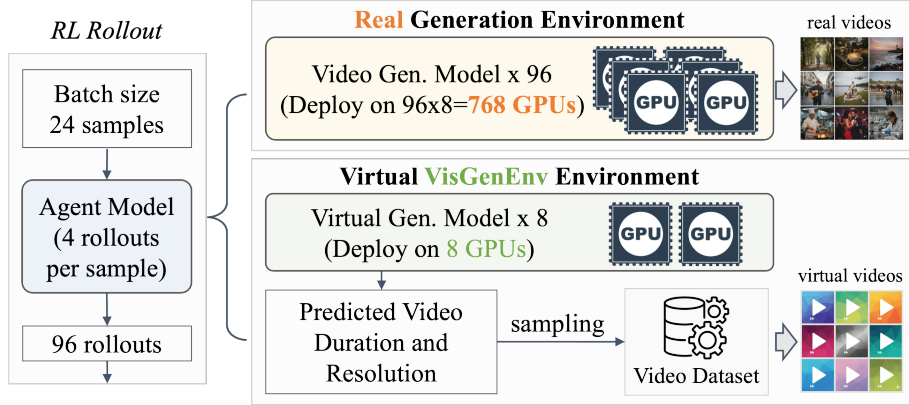


Figure 7: Comparison of the real environment and our virtual VisGenEnv environment, with an example of using a video generation tool.

reward design and theoretical analysis. VisGenEnv integrates a comprehensive suite of 36 *visual creation tools* (see Appendix for full list). The core of its design lies in a procedural simulation that accurately replicates the functional logic and behavioral patterns of real tools, including state transitions, parameter validation, and output specifications such as image resolution and video duration. To simulate multimodal outputs, the environment returns media files randomly sampled from a database while ensuring physically correct attributes consistent with tool specifications. This high-fidelity simulation of tool behaviors enables the agent to effectively learn the causal structure of the workflow and master robust planning policies through extensive practice within the virtual setting.

Training agent models by reinforcement learning in the real environment is prohibitively expensive. As illustrated in Fig. 7, supporting a training batch size of 24 with 4 rollouts (i.e., 96 concurrent rollouts in total) quickly becomes computationally intractable. Video tools are particularly costly: each instance requires 8 GPUs and roughly 30 seconds per video, meaning 96 concurrent rollouts would require  $8 \times 96 = 768$  GPUs. Deploying multiple real image and video generation tools would require several thousand GPUs, while our virtual environment VisGenEnv enables long-horizon exploration with only a few GPUs—thus saving thousands of GPU resources.

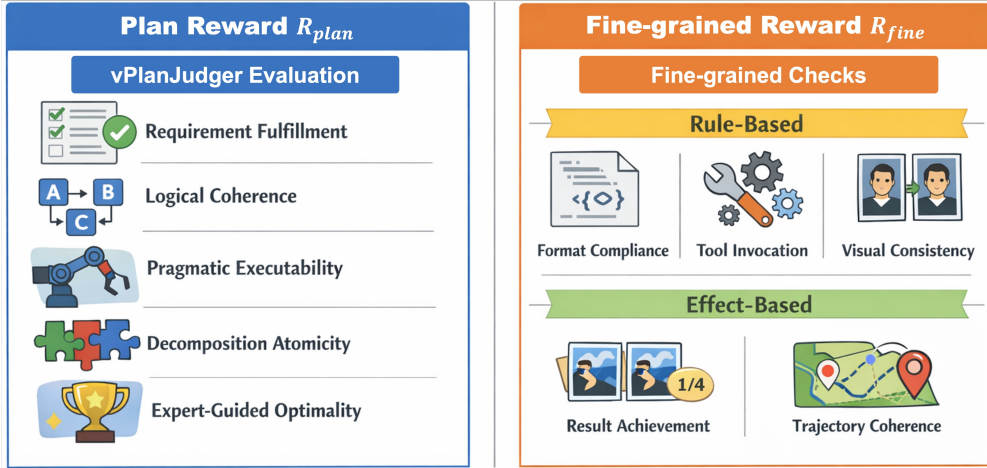


Figure 8: LtrReward Components.

### 4.3.2 LtrReward Components

With the virtual environment in place, as shown in Fig. 8, we now define LtrReward components  $R_{vrt}$  (i.e., virtual reward applicable to VisGenEnv) as reward signals that guide the agent’s learning, which consist of Plan Reward  $R_{plan}$  and Fine-grained Reward  $R_{fine}$ .

Plan Reward  $R_{plan}$  evaluates the overall quality of the task plan using a proposed **vPlanJuder**, an expert-informed LLM evaluator that leverages a curated repository of expert reference plans to provide in-context guidance. By performing cross-referenced reasoning between the candidate

plan and expert-authored strategies, the vPlanJudger computes a multidimensional alignment score focusing on five key facets: (1) *Requirement Fulfillment*, a binary check on whether the output’s modality and quantity align with the user request; (2) *Logical Coherence*, verifying the causal validity of sub-task sequencing; (3) *Pragmatic Executability*, ensuring each step is grounded within the available toolset or LLM capabilities to avoid hallucinatory actions; (4) *Decomposition Atomicity*, which evaluates whether the plan is partitioned into actionable atomic tasks; and (5) *Expert-Guided Optimality*, which rewards task-specific best practices such as identity consistency for multi-shot content, beat-aligned audio-visual synchronization, and the strategic minimization of complexity.

The Fine-grained Reward  $R_{\text{fine}}$  integrates both rule-based and effect-based signals to ensure structurally valid execution and successful task realization. Specifically: (1) Rule-based components include Format Compliance  $R_{\text{format}}$ , which validates UTPC structural correctness via parsing of tags, ordering, content, and JSON validity; Tool Invocation  $R_{\text{tool}}$ , which scores execution success with graded penalties for intermediate or final failures; and Visual Consistency  $R_{\text{cons}}$ , which rewards appropriate use of reference-based generation when consistency is required. (2) Effect-based components include Result Achievement  $R_{\text{result}}$ , which verifies output constraints such as image count and video duration within tolerance bounds, and Trajectory Coherence  $R_{\text{traj}}$ , which evaluates alignment between planning intent and executed actions through an LLM-evaluator. Together, these rewards provide trajectory-level supervision that encourages correct agentic structure, reliable tool usage, and coherent visual creation outcomes.

### 4.3.3 Theoretical Foundations of Virtual Reinforcement Learning

Based on the constructed virtual environment and the LtrReward components, we provide a theoretical analysis to explain the effectiveness of VRL when transferred to real-world execution. The theoretical legitimacy of VRL rests on its ability to maintain policy efficacy despite the intrinsic discrepancies between virtual simulation and real-world execution. Specifically, VRL operates under a **Rollout Gap**, where the agent lacks real visual feedback to rectify its trajectory, and an **Objective Inconsistency**, caused by substituting the vision reward  $R_{\text{vision}}$  (which measures perceptual quality across multiple visual dimensions) with a structural proxy  $R_{\text{result}}$ . To evaluate how these discrepancies affect policy transfer, we model the sim-to-real transition as a function of four synergistic variables: (i) **Tool Capability** ( $C_{\text{tool}}$ ), quantifying the reliability of the generative engine; (ii) **PST Prior** ( $\pi_{\text{pst}}$ ), anchoring the agent’s initial reasoning within a distribution derived from real expert data; (iii) **Plan Sufficiency** ( $\Phi_{\text{plan}}$ ), measuring the causal link between logical correctness and visual quality; and (iv) **Result Reward** ( $R_{\text{result}}$ ), ensuring the structural completion of tasks.

The following theorems establish the mathematical foundation of VRL: Theorem 4.1 provides an error bound guarantee, proving that the sim-to-real gap remains controllable under the joint constraint of these variables; Theorem 4.2 characterizes the real-world performance gain as a competition between *Causal Improvement* and *Transfer Loss*, showing that VRL yields non-negative improvement whenever the causal reward gain dominates the bounded sim-to-real error.

**Theorem 4.1** (Virtual-to-Real Error Bound). *Let  $J_{\text{real}}(\pi)$  and  $J_{\text{vrt}}(\pi)$  be the expected returns of policy  $\pi$  in real and virtual environments. And  $\delta, \alpha, \beta$  are environment-specific scaling factors. The transfer error  $\mathcal{E}(\pi) = |J_{\text{real}}(\pi) - J_{\text{vrt}}(\pi)|$  is bounded by:*

$$\mathcal{E}(\pi) \leq \underbrace{\delta(1 - C_{\text{tool}})}_{\text{Dynamics Gap}} + \underbrace{\alpha \cdot D_{\text{KL}}(\pi_{\text{vrt}}|\pi_{\text{pst}})}_{\text{Action Bias Bound}} + \underbrace{\beta(1 - \Phi_{\text{plan}} \cdot R_{\text{result}})}_{\text{Goal Alignment Error}} \quad (5)$$

Theorem 4.1 quantifies how the sim-to-real divergence is suppressed: (i) *Dynamics Gap* is minimized by  $C_{\text{tool}}$ , ensuring virtual procedural logic mirrors real API behavior; (ii) *Action Bias Bound* is constrained by the PST prior, which prevents policy drift in the absence of real visual feedback by maintaining consistency with expert decision-making; (iii) *Goal Alignment Error* is mitigated by the coupling of  $\Phi_{\text{plan}}$  and  $R_{\text{result}}$ , ensuring the virtual completion objective serves as a reliable proxy for real-world success.

**Theorem 4.2** (Real-World Improvement of VRL). *Under the error bound  $\mathcal{E}$ , the real-world performance gain depends on the dominance of Causal Improvement over Transfer Loss:*

$$J_{\text{real}}(\pi_{\text{VRL}}) - J_{\text{real}}(\pi_{\text{pst}}) \geq \underbrace{\Gamma \cdot \mathbb{E}_{\pi}[\Delta R_{\text{vrt}}]}_{\text{Causal Improvement}} - \underbrace{\mathcal{E}(\pi)}_{\text{Transfer Loss}} \quad (6)$$

where  $\Gamma = C_{\text{tool}} \cdot \Phi_{\text{plan}} \cdot \kappa(\pi_{\text{pst}})$  is the effectiveness coefficient, and  $\kappa(\pi_{\text{pst}})$  denotes the anchoring strength of the PST prior in constraining policy exploration. Virtual reward  $R_{\text{vrt}}$  consisting of  $R_{\text{plan}}$  and  $R_{\text{fine}}$ , and  $\mathbb{E}_{\pi}[\Delta R_{\text{vrt}}]$  denotes the expected increment of virtual reward, representing the agent’s logic optimization in planning and execution.

The practical transferability of VRL is validated by the convergence behavior in our experiments, where the agent achieves an average virtual reward exceeding 95%. This saturation of total virtual reward  $R_{\text{vrt}}$  indicates that the **Causal Improvement** term is maximized, providing a substantial logical buffer to offset transfer discrepancies. By substituting these empirical results into Theorem 4.1, we observe that the *Action Bias Bound* is strictly suppressed by the PST prior, while the *Goal Alignment Error* is mitigated by the coupling of  $\Phi_{\text{plan}}$  and  $R_{\text{result}}$ , remaining stable as the agent masters structural completion. Consequently, the **Transfer Loss**  $\mathcal{E}(\pi)$  is primarily governed by the *Dynamics Gap*  $\delta(1 - C_{\text{tool}})$ . This reveals a critical insight: VRL efficacy is fundamentally a function of generative tool quality. As  $C_{\text{tool}}$  increases—meaning the underlying visual creation tools become more reliable and follow procedural logic more closely—the transfer loss diminishes, allowing the massive logical gains from virtual training to translate effectively into superior real-world visual quality. Therefore, we derive the following corollary:

**Corollary 4.3** (Fidelity-Anchored Transfer). *Provided the virtual reward  $R_{\text{vrt}}$  reaches a near-optimal level, the real-world gain of VRL is monotonically non-decreasing with respect to  $C_{\text{tool}}$ .*

#### 4.3.4 Plan-Driven Reward Design

Theorems 4.1 and 4.2 indicate that real-world improvement critically depends on planning quality. Motivated by this insight, we adopt a plan-driven reward that enforces causal dependency between planning and execution:

$$R_{\text{vrt}} = R_{\text{plan}} \times R_{\text{fine}} [R_{\text{tool}} + R_{\text{format}} + R_{\text{result}} + R_{\text{traj}} + R_{\text{cons}}]. \quad (7)$$

Here,  $R_{\text{plan}}$  measures plan correctness, while  $R_{\text{fine}}$  captures execution-level structural validity. The multiplicative coupling ensures that execution alone cannot achieve high reward without a valid plan, and maximal reward is obtained only when a correct plan is faithfully executed. This mechanism directly aligns with Theorem 4.2, promoting robust long-horizon planning and tool-use strategies within virtual training.

## 5 Experiment

### 5.1 VisGenBench

Existing video generation benchmark VBench-2.0 Zheng et al. (2025) has made significant contributions to evaluating the quality of individual-generated videos. But it lacks the capability to evaluate *multi-step visual creation trajectories* that involve complex tool invocation and long-horizon planning. While ComfyBench Xue et al. (2025) attempts to assess multi-step trajectories, it is specifically designed for ComfyUI comfyanonymous (2023) and evaluates agent performance based solely on ComfyUI execution success, making it unsuitable for general API-based tool invocation scenarios. To address this critical gap, we introduce **VisGenBench**, a comprehensive benchmark designed for evaluating *visual generation agentic models* that operate through multi-step tool invocation to accomplish complex image and video creation tasks.

Table 1: Test dataset composition of VisGenBench, with 400 image tasks and 800 video tasks.

Type	Content Creative	Content Match	Object Consistency	Scene Consistency	Style Consistency	Variety	Visual Amount	Video Duration	Video Storyboard
Image Tasks	50	50	50	50	50	50	100	–	–
Video Tasks	50	50	50	50	50	50	100	200	200
<b>Total</b>	100	100	100	100	100	100	200	200	200

#### 5.1.1 Test Dataset Composition

As shown in Tab. 1, the VisGenBench consists of a total of 1.2k test samples, including 400 image-generation tasks and 800 video-generation tasks. Each task is designed to reflect multi-step

creation trajectories, requiring to generation of many images and videos. The benchmark spans 10 evaluation dimensions and covers 35+ real-world application scenarios, encompassing domains such as advertising, storytelling, entertainment, animation, etc.

### 5.1.2 Evaluation Framework

The VisGenBench evaluation framework integrates both objective and subjective assessments to measure an agent’s ability to perform multi-step visual generation tasks.

**Objective Evaluation** Objective evaluation focuses on quantifiable and automatically measurable aspects of the generated content. Specifically, it consists of two components: (1) *Success Rate*: Measures whether the model successfully returns valid images/videos when requested by user. A generation containing the correct modality is counted as *Success*. (2) *Basic Visual Attributes*: Quantitative evaluation of the generated results, including visual quantity, video storyboard count, and video duration. These attributes are automatically assessed using standardized tools.

**Subjective Evaluation** Subjective aspects such as visual consistency, diversity, storytelling quality, and audio perception cannot be fully captured through traditional metrics. We therefore introduce a VLM-Grader with pre-defined fine-grained scoring rubrics, implemented using the Gemini2.5-Pro model. For each subjective evaluation dimension, we define a tailored *meta evaluation list*—a structured rubric containing detailed scoring items (e.g., character consistency, style coherence, narrative flow, audio synchronization, etc). Gemini2.5-Pro provides a meta-evaluation score for each meta-item, and the aggregated score forms the overall result for that dimension. To align automated scoring with human judgment, we calibrate Gemini2.5-Pro’s meta-evaluation intensity on VisGenBench. This ensures that both mean scores and relative rankings evaluated by Gemini2.5-Pro remain consistent with expert human assessments, achieving a human-aligned evaluation process.

Table 2: Comparisons on VisGenBench by VLM Evaluation. S-Rate: Success Rate, O-Score: Overall Score. The **best** and **second-best** results are highlighted.

Method	Creative Match	Object Scene	Style Variety	Amount	Duration	Storyboard	S-Rate	O-Score			
GPT-5	0.683	0.641	0.593	0.579	<b>0.638</b>	0.232	<b>0.620</b>	0.263	0.660	0.863	0.577
Gemini2.5-Pro	<b>0.777</b>	<b>0.802</b>	0.625	0.602	0.573	<b>0.345</b>	0.540	0.376	<b>0.700</b>	<b>0.933</b>	<b>0.627</b>
Qwen3-VL-8B-Tk	0.104	0.078	0.100	0.065	0.109	0.014	0.160	0.034	0.040	0.142	0.085
<b>VisionCreator-8B</b>	0.651	0.661	<b>0.645</b>	<b>0.638</b>	0.595	0.211	0.480	<b>0.429</b>	0.580	<b>0.925</b>	<b>0.581</b>

Table 3: Comparisons on VisGenBench by Human Evaluation. All models use the new version system prompt, which differs from Tab.2. Overall Score = (Success Rate of Image × Human Evaluation of Image + Success Rate of Video × Human Evaluation of Video)/2. The performance comparisons of all detailed human evaluation dimensions are shown in Fig. 1.

Model	Success Rate		Human Evaluation		Overall Score
	Image	Video	Image	Video	
GPT-5	95.95%	93.00%	3.52	3.25	3.19
Gemini2.5-Pro	91.00%	84.00%	3.53	3.35	3.01
Qwen3-VL-32B-Thinking	97.00%	93.00%	3.47	3.23	3.18
Qwen3-VL-32B-RL	91.00%	87.00%	3.51	3.40	3.07
Qwen3-VL-32B-SFT	96.00%	94.00%	3.53	3.37	3.27
VisionCreator-32B	<b>99.00%</b>	<b>96.00%</b>	<b>3.53</b>	<b>3.49</b>	<b>3.42</b>

## 5.2 Results on VisGenBench by VLM Evaluation

As shown in Tab. 2, our VisionCreator-8B demonstrates remarkable performance that is highly competitive with much larger commercial models (GPT-5 and Gemini2.5-Pro), while significantly outperforming its base model Qwen3-VL-8B-Thinking. The key findings highlight several advantages of our approach: (1) *Superior Success Rate and Reliability*: VisionCreator-8B achieves an impressive success rate of 0.925, surpassing GPT-5 (0.863) and approaching Gemini2.5-Pro (0.933). This demonstrates the effectiveness of our UTPC framework in ensuring task completion reliability, a crucial requirement for practical visual creation applications. (2) *Exceptional Consistency Performance*: VisionCreator-8B achieves the highest scores in object consistency (0.645) and scene

Table 4: Ablation study with VisionCreator-8B on VisGenBench-104 comparing different training strategies. VisGenBench-104 is a sampled subset of VisGenBench. Model configurations: **RL1**: PST + Result+Format reward; **RL2**: PST + Plan×(Result+Format) reward; **RL3**: Qwen3-VL + Plan×(Result+Format) reward; **RL4**: PST + Plan×Fine reward; **v1**: 3×VisGenData-4k; **v2**: 3×VisGenData-4k + General-1M; **v3**: 20×VisGenData-4k + General-1M; **v4**: PST + 3×VisGenData-4k + General-1%; **v5**: PST + 3×VisGenData-4k + General-5%; **v6**: PST + 3×VisGenData-4k + General-10%; **v7**: PST + 3×VisGenData-4k + General-20%.

Method	Creative	Match	Object	Scene	Style	Variety	Amount	Duration	Storyboard	S-Rate	O-Score
<b>RL1</b>	0.534	<b>0.817</b>	<b>0.694</b>	0.547	<b>0.579</b>	0.249	<b>1.000</b>	0.397	0.625	0.904	0.634
<b>RL2</b>	0.579	0.808	0.677	0.479	0.558	<b>0.265</b>	0.800	0.478	<b>0.875</b>	0.942	0.644
<b>RL3</b>	<b>0.671</b>	0.674	0.621	0.622	0.555	0.217	0.800	0.513	0.750	0.885	0.631
<b>RL4</b>	0.573	0.794	0.672	<b>0.696</b>	0.569	0.150	<b>1.000</b>	<b>0.534</b>	0.625	0.925	0.654
<b>v1</b>	0.000	0.050	0.000	0.000	0.000	0.000	0.000	0.000	0.000	0.019	0.007
<b>v2</b>	0.230	0.334	0.382	0.339	0.396	0.163	0.600	0.134	0.500	0.490	0.357
<b>v3</b>	0.262	0.422	0.300	0.260	0.473	0.068	0.600	0.100	0.250	0.481	0.322
<b>v4</b>	0.283	0.468	0.399	0.295	0.318	0.000	0.600	0.183	0.000	0.442	0.299
<b>v5</b>	0.266	0.361	0.366	0.246	0.201	0.084	0.200	0.029	0.125	0.490	0.237
<b>v6</b>	0.239	0.310	0.326	0.194	0.273	0.149	0.600	0.098	0.125	0.413	0.273
<b>v7</b>	0.420	0.701	0.430	0.447	0.430	0.028	0.600	0.344	0.375	0.625	0.440

consistency (0.638) among all compared models, including the much larger Gemini2.5-Pro and GPT-5. This validates our model’s strong capability in maintaining visual coherence throughout multi-step creation processes, a core benefit of the native agentic architecture. (3) The results validate our core hypothesis: a specialized native visual creation agent, even with significantly fewer parameters, can achieve performance competitive with general-purpose commercial giants through targeted architectural design and training methodology. VisionCreator’s particular strengths in success rate and consistency metrics underscore the practical advantages of our UTPC framework for real-world visual content creation applications.

### 5.3 Results on VisGenBench by Human Evaluation

In addition to automated VLM-based evaluation (Tab. 2), we conduct a thorough *human evaluation* to assess the perceptual quality of multi-step visual creation tasks, including images and videos (Tab. 3), which shows that: (1) **Overall Findings**: VisionCreator-32B achieves the highest Overall Score of 3.42, surpassing both GPT-5 (3.19) and Gemini2.5-Pro (3.01). This indicates that our UTPC framework not only ensures task success in an automated setting but also delivers outputs that are qualitatively preferred by human evaluators. (2) **Image vs. Video Performance**: VisionCreator-32B excels across both modalities, with 99% image success and 96% video success, accompanied by strong human evaluation scores (3.53 for images, 3.49 for videos). This balanced performance highlights the model’s capability to maintain coherent multi-step planning and execution for both static and dynamic content. (3) **Implications**: The human evaluation corroborates trends observed in VLM-based metrics, validating that the model’s planning-driven reward design and VRL training not only improve automated success metrics but also enhance perceptual quality, consistency, and user satisfaction in real-world multi-step visual creation tasks.

### 5.4 Ablation Studies

We conduct ablation studies on sampled VisGenBench-104, where key findings from Tab. 4 include: (1) **Effectiveness of PST**. Our PST with *v7* (*PST + 3×VisGenData-4k + General-20%*) achieves significant improvement over SFT with *v2* (*3×VisGenData-4k + General-1M*) (0.440 vs. 0.357). Performance improves with increasing general data ratio (*v4*→*v5*→*v6*→*v7*), confirming balanced specialization prevents overfitting while maintaining generalization. (2) **Data Configuration Strategies**. Simply increasing specialized data scale does not guarantee improvement. *v3* (*20×VisGenData-4k + General-1M*) underperforms *v2* (*3×VisGenData-4k + General-1M*) (0.322 vs. 0.357), indicating excessive data repetition causes overfitting. Our PST strategy achieves better performance through optimized data ratios. (3) **Virtual Reinforcement Learning**. All VRL models substantially outperform SFT variants. *RL4* (*PST + Plan×Fine reward*) improves Overall Score by 49% over the best PST model *v7* (0.654 vs. 0.440), demonstrating VRL’s effectiveness. (4) **Reward Function Designs**. Building upon *RL1*, *RL2* (*PST + Plan×(Result+Format) reward*) which incorporates additional plan reward, demon-

strates improved performance with a higher Success Rate (0.942 vs. 0.904) and Overall Score (0.644 vs. 0.634). *RL4* achieves the best Overall Score (0.654) and demonstrates strong comprehensive performance across multiple dimensions, proving fine-grained rewards enhance model capability. (5) **Importance of Pre-training Foundation** *RL2* ( $PST + Plan \times (Result + Format)$  reward) outperforms *RL3* ( $Qwen3-VL + Plan \times (Result + Format)$  reward) (0.644 vs. 0.631) despite identical rewards, with *RL2* achieving a notably higher Success Rate of 0.942 compared to 0.885 for *RL3*, validating *PST* provides a stronger foundation for RL training.

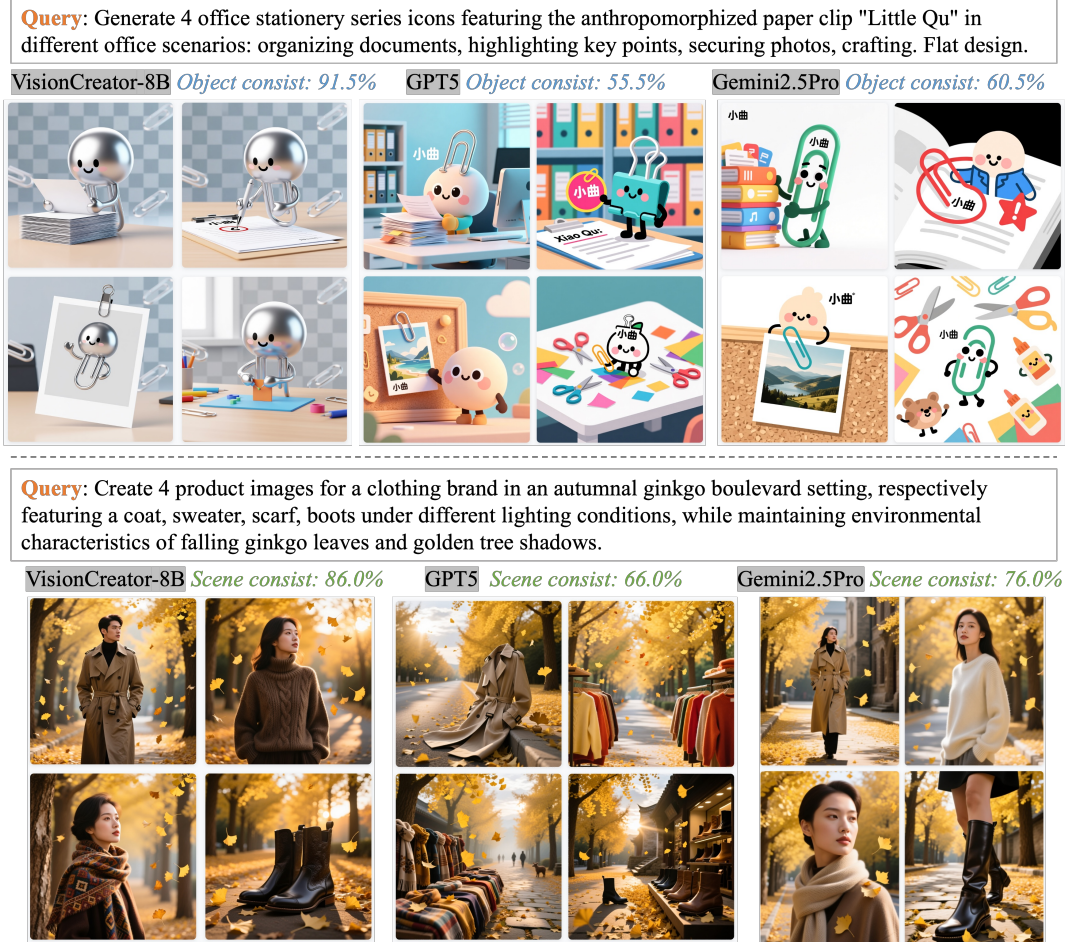


Figure 9: Visualization comparisons of consistency.

## 6 Conclusion

We present VisionCreator, a native visual-generation agent that unifies Understanding, Thinking, Planning, and Creation (UTPC) in an end-to-end framework. Our contributions include: (1) VisGenData-4k with UTPC structures via metacognition-based VisionAgent; (2) Progressive Specialization Training and Virtual Reinforcement Learning for stable capability acquisition; (3) VisGenBench for multi-step visual creation evaluation. Experiments show VisionCreator outperforms larger closed-source models, validating our approach. This work establishes a foundation for visual-generation agentic systems and autonomous creative content generation.

---

## Detailed Theoretical Derivations of VRL Theorems

This appendix provides detailed mathematical derivations and proofs for the two VRL theorems presented in the main text. The derivation process is divided into three stages: formal modeling and definitions, derivation of the error upper bound (Theorems 4.1), and analysis of performance improvement (Theorems 4.2).

### Stage 1: Formal Modeling and Definitions

We first formalize the agent’s policy, environment, and rewards to establish the foundation for subsequent derivations.

#### 1.1 Formalization of Environment and Policy

**Definition A.1 (MDP Tuple):** The real-world task is modeled as a Markov Decision Process (MDP), denoted as  $\mathcal{M}_{\text{real}} = (\mathcal{S}, \mathcal{A}, P_{\text{real}}, R_{\text{vision}}, \rho_0, \gamma)$ .

- $\mathcal{S}$ : State space, containing multimodal observations  $o_t$  (textual instructions, tool feedback, virtual visual states).
- $\mathcal{A}$ : Action space, containing reasoning tokens, planning steps, and tool invocations.
- $P_{\text{real}}(s'|s, a)$ : Dynamic transition probability of the real environment.
- $R_{\text{vision}}(s, a, s')$ : Real reward function, measuring the perceptual quality of generated content (e.g., aesthetics, alignment).
- $\rho_0$ : Initial state distribution.
- $\gamma \in (0, 1)$ : Discount factor.

**Definition A.2 (Virtual Environment):** The virtual environment is  $\mathcal{M}_{\text{vrt}} = (\mathcal{S}, \mathcal{A}, P_{\text{vrt}}, R_{\text{vrt}}, \rho_0, \gamma)$ . Its core differences are:

- $P_{\text{vrt}}(s'|s, a)$ : Tool dynamics simulated by VisGenEnv, with fidelity quantified by the **tool capability**  $C_{\text{tool}} \in [0, 1]$ .
- $R_{\text{vrt}}$ : Virtual reward function, composed of  $R_{\text{plan}}$  and  $R_{\text{fine}}$  according to the plan-driven reward design. It is a structural proxy reward that substitutes for the computationally infeasible  $R_{\text{vision}}$  in the virtual environment.

**Definition A.3 (Policy and Return):** Let  $\pi$  be a policy (mapping from states to actions). The expected discounted return of policy  $\pi$  in environment  $\mathcal{M}$  is defined as:

$$J(\pi; \mathcal{M}) = \mathbb{E}_{\tau \sim (\pi, \mathcal{M})} \left[ \sum_{t=0}^{\infty} \gamma^t R(s_t, a_t, s_{t+1}) \right].$$

Here, the trajectory  $\tau = (s_0, a_0, s_1, a_1, \dots)$  is generated by  $s_0 \sim \rho_0$ ,  $a_t \sim \pi(\cdot|s_t)$ , and  $s_{t+1} \sim P(\cdot|s_t, a_t)$ . For brevity, we denote  $J_{\text{real}}(\pi) = J(\pi; \mathcal{M}_{\text{real}})$  and  $J_{\text{vrt}}(\pi) = J(\pi; \mathcal{M}_{\text{vrt}})$ .

#### 1.2 Key Variables and Core Assumptions

**Definition A.4 (Key Variables):**

- **Tool capability**  $C_{\text{tool}}$ : Measures how well the virtual environment dynamics  $P_{\text{vrt}}$  approximate the real dynamics  $P_{\text{real}}$ .  $C_{\text{tool}} = 1$  indicates perfect simulation.
- **PST prior**  $\pi_{\text{pst}}$ : The initialization policy obtained through Progressive Specialization Training (PST). Its behavioral distribution on real expert data is denoted as  $d_{\text{pst}}(s, a)$ .
- **Plan sufficiency**  $\Phi_{\text{plan}} \in [0, 1]$ : Measures the strength of the causal link between a “logically correct” plan and the final “high-quality visual output”.
- **Result reward**  $R_{\text{result}} \in [0, 1]$ : A subcomponent of  $R_{\text{fine}}$  that evaluates whether the task is structurally completed (e.g., number of images, video duration).

---

**Assumption A.1 (Dynamic Difference Upper Bound):** There exists a constant  $\delta > 0$  related to environment complexity such that for all state-action pairs  $(s, a)$ ,

$$|P_{\text{real}}(\cdot|s, a) - P_{\text{vrt}}(\cdot|s, a)|_1 \leq \delta(1 - C_{\text{tool}}).$$

This assumption stems from the high-fidelity simulation design of VisGenEnv: higher tool capability  $C_{\text{tool}}$  leads to smaller differences between virtual and real transitions.

**Assumption A.2 (Reward Proxy Error):** The relationship between the real visual reward  $R_{\text{vision}}$  and the proxy reward is modulated by plan sufficiency  $\Phi_{\text{plan}}$  and result reward  $R_{\text{result}}$ . There exists a constant  $\beta > 0$  such that for meaningful trajectories (i.e., when planning logic is correct), the reward difference satisfies:

$$|R_{\text{vision}}(s, a, s') - \Phi_{\text{plan}} \cdot R_{\text{result}}(s, a, s')| \leq \beta(1 - \Phi_{\text{plan}} \cdot R_{\text{result}}).$$

This assumption reflects the design philosophy of LtrReward: when planning is sufficient ( $\Phi_{\text{plan}} \approx 1$ ) and the task is perfectly completed structurally ( $R_{\text{result}} \approx 1$ ), the real visual quality also tends to be high.

**Assumption A.3 (KL Constraint on Policy Deviation):** The policy  $\pi_{\text{vrt}}$  trained in the virtual environment differs from the PST prior  $\pi_{\text{pst}}$  in the state-action distribution. This difference can be measured by the KL divergence  $D_{\text{KL}}(\pi_{\text{vrt}}|\pi_{\text{pst}})$ , and its impact on the return difference is linearly bounded. That is, there exists a constant  $\alpha > 0$  such that the related performance difference is constrained by it.

**Definition A.5 (Sim-to-Real Error):** For a given policy  $\pi$ , its sim-to-real error is defined as:

$$\mathcal{E}(\pi) = |J_{\text{real}}(\pi) - J_{\text{vrt}}(\pi)|.$$

## Stage 2: Derivation of Theorems 4.1 (Virtual-to-Real Error Upper Bound)

**Theorems 4.1 (Virtual-to-Real Error Upper Bound) Restated:** Under Assumptions A.1, A.2, A.3, for any policy  $\pi$  (trained in the virtual environment, denoted as  $\pi_{\text{vrt}}$ ), its sim-to-real error  $\mathcal{E}(\pi)$  satisfies:

$$\mathcal{E}(\pi) \leq \underbrace{\delta(1 - C_{\text{tool}})}_{\text{Dynamics Gap}} + \underbrace{\alpha \cdot D_{\text{KL}}(\pi_{\text{vrt}}|\pi_{\text{pst}})}_{\text{Action Bias Bound}} + \underbrace{\beta(1 - \Phi_{\text{plan}} \cdot R_{\text{result}})}_{\text{Goal Alignment Error}}.$$

**Proof:**

We decompose the total error into three separately bounded components via the triangle inequality and constrain each using the above assumptions.

**Step 2.1: Decompose Total Error** Consider an intermediate environment  $\mathcal{M}_{\text{hybrid}} = (\mathcal{S}, \mathcal{A}, P_{\text{vrt}}, R_{\text{vision}}, \rho_0, \gamma)$ , which uses the virtual environment dynamics  $P_{\text{vrt}}$  but retains the real reward  $R_{\text{vision}}$ . Denote  $J_{\text{hybrid}}(\pi) = J(\pi; \mathcal{M}_{\text{hybrid}})$ . Then:

$$\begin{aligned} \mathcal{E}(\pi) &= |J_{\text{real}}(\pi) - J_{\text{vrt}}(\pi)| \\ &\leq |J_{\text{real}}(\pi) - J_{\text{hybrid}}(\pi)| \quad (\text{Term I: Dynamics Gap}) \\ &\quad + |J_{\text{hybrid}}(\pi) - J_{\text{vrt}}^{\text{ideal}}(\pi)| \quad (\text{Term II: Reward Gap}) \\ &\quad + |J_{\text{vrt}}^{\text{ideal}}(\pi) - J_{\text{vrt}}(\pi)|. \quad (\text{Term III: Policy Bias}) \end{aligned}$$

Here  $J_{\text{vrt}}^{\text{ideal}}(\pi)$  represents the ideal return under dynamics  $P_{\text{vrt}}$  and reward  $R_{\text{vision}}$  with the policy perfectly constrained by the PST prior (no deviation). We next upper bound each term.

**Step 2.2: Bounding Term I (Dynamics Gap)** Term I measures the return difference due to the difference between dynamic models  $P_{\text{real}}$  and  $P_{\text{vrt}}$ . According to **Assumption A.1** and the **Performance Difference Lemma**, for any policy  $\pi$ ,

$$|J_{\text{real}}(\pi) - J_{\text{hybrid}}(\pi)| \leq \frac{\gamma \cdot \delta(1 - C_{\text{tool}})}{(1 - \gamma)^2} \cdot \max_{s,a} |R_{\text{vision}}(s, a)|.$$

Let  $R_{\text{max}} = \max_{s,a} |R_{\text{vision}}(s, a)|$  and define  $\delta' = \frac{\gamma R_{\text{max}}}{(1 - \gamma)^2} \delta$ , we obtain:

$$\text{Term I} \leq \delta'(1 - C_{\text{tool}}).$$

In the theorem statement, constant factors are absorbed into  $\delta$ , so we have Term I  $\leq \delta(1 - C_{\text{tool}})$ .

**Step 2.3: Bounding Term II (Reward Gap)** Term II measures the difference between using the real reward  $R_{\text{vision}}$  and using the proxy reward  $\Phi_{\text{plan}} \cdot R_{\text{result}}$  (as the core part of  $R_{\text{vrt}}$ ) under the same dynamics. According to **Assumption A.2**, for each step in the trajectory, the reward difference is bounded. Applying the Performance Difference Lemma (reward difference part) again yields:

$$|J_{\text{hybrid}}(\pi) - J_{\text{vrt}}^{\text{ideal}}(\pi)| \leq \frac{\beta(1 - \Phi_{\text{plan}} \cdot R_{\text{result}})}{1 - \gamma}.$$

Define  $\beta' = \beta/(1 - \gamma)$ , then Term II  $\leq \beta'(1 - \Phi_{\text{plan}} \cdot R_{\text{result}})$ . In the theorem statement,  $\beta'$  is written as  $\beta$ .

**Step 2.4: Bounding Term III (Policy Bias)** Term III measures the return loss due to the deviation of the virtually trained policy  $\pi_{\text{vrt}}$  from the ideal PST prior  $\pi_{\text{pst}}$ . According to **Assumption A.3**, there exists a constant  $\alpha > 0$  such that:

$$|J_{\text{vrt}}^{\text{ideal}}(\pi) - J_{\text{vrt}}(\pi)| \leq \alpha \cdot D_{\text{KL}}(\pi_{\text{vrt}}|\pi_{\text{pst}}).$$

This assumption stems from the ‘‘anchoring’’ effect of the PST prior on the policy exploration space, preventing catastrophic policy drift in the absence of real visual feedback.

**Step 2.5: Combining Error Upper Bounds** Summing the upper bounds of Term I, II, and III, we obtain:

$$\mathcal{E}(\pi) \leq \delta'(1 - C_{\text{tool}}) + \beta'(1 - \Phi_{\text{plan}} \cdot R_{\text{result}}) + \alpha \cdot D_{\text{KL}}(\pi_{\text{vrt}}|\pi_{\text{pst}}).$$

Relabeling constants  $\delta' \rightarrow \delta$ ,  $\beta' \rightarrow \beta$  yields the form in Theorems 4.1. ■

### Stage 3: Derivation of Theorems 4.2 (Real-World Performance Improvement Lower Bound)

**Theorems 4.2 (Real-World Improvement of VRL)** Restated: Let  $\pi_{\text{pst}}$  be the initial policy after PST training, and  $\pi_{\text{VRL}}$  be the policy optimized through Virtual Reinforcement Learning (VRL). Define the virtual optimization gain as  $\Delta_{\text{vrt}} = J_{\text{vrt}}(\pi_{\text{VRL}}) - J_{\text{vrt}}(\pi_{\text{pst}}) = \mathbb{E}_{\pi}[\Delta(R_{\text{plan}} + R_{\text{fine}})]$ . Then, under the error bound of Theorems 4.1, the real-world performance improvement satisfies:

$$J_{\text{real}}(\pi_{\text{VRL}}) - J_{\text{real}}(\pi_{\text{pst}}) \geq \underbrace{\Gamma \cdot \Delta_{\text{vrt}}}_{\text{Causal Improvement}} - \underbrace{\mathcal{E}(\pi_{\text{VRL}})}_{\text{Transfer Loss}},$$

where  $\Gamma = C_{\text{tool}} \cdot \Phi_{\text{plan}} \cdot \kappa(\pi_{\text{pst}})$  is the effectiveness coefficient, and  $\kappa(\pi_{\text{pst}}) \in (0, 1]$  denotes the **Anchoring Strength** of the PST prior in constraining policy exploration.

**Proof:**

**Step 3.1: Establish Inequality Based on Error Bound** From Theorems 4.1, for any policy  $\pi$ , we have  $J_{\text{real}}(\pi) \geq J_{\text{vrt}}(\pi) - \mathcal{E}(\pi)$ . Applying this inequality to  $\pi_{\text{VRL}}$  and  $\pi_{\text{pst}}$  respectively:

$$\begin{aligned} J_{\text{real}}(\pi_{\text{VRL}}) &\geq J_{\text{vrt}}(\pi_{\text{VRL}}) - \mathcal{E}(\pi_{\text{VRL}}), \\ J_{\text{real}}(\pi_{\text{pst}}) &\geq J_{\text{vrt}}(\pi_{\text{pst}}) - \mathcal{E}(\pi_{\text{pst}}). \end{aligned}$$

Subtracting the second inequality from the first yields:

$$J_{\text{real}}(\pi_{\text{VRL}}) - J_{\text{real}}(\pi_{\text{pst}}) \geq [J_{\text{vrt}}(\pi_{\text{VRL}}) - J_{\text{vrt}}(\pi_{\text{pst}})] - [\mathcal{E}(\pi_{\text{VRL}}) - \mathcal{E}(\pi_{\text{pst}})].$$

Since  $\pi_{\text{pst}}$  itself is trained on real expert data, its sim-to-real error  $\mathcal{E}(\pi_{\text{pst}})$  is expected to be small (aligned during PST). Therefore, the lower bound of performance improvement is mainly affected by the error  $\mathcal{E}(\pi_{\text{VRL}})$  of  $\pi_{\text{VRL}}$ . Conservatively setting the transfer loss term as  $\mathcal{E}(\pi_{\text{VRL}})$  gives:

$$J_{\text{real}}(\pi_{\text{VRL}}) - J_{\text{real}}(\pi_{\text{pst}}) \geq \Delta_{\text{vrt}} - \mathcal{E}(\pi_{\text{VRL}}). \quad (1)$$

**Step 3.2: Relating Virtual Gain to Real Gain (Causal Improvement)** The  $\Delta_{\text{vrt}}$  in inequality (1) is the gain in virtual reward. We need to relate it to real performance improvement. This relies on a core idea: optimizing ‘‘planning and execution logic’’ in the virtual environment, as long as the simulation is sufficiently credible, causally leads to improved real-world visual quality. Define the **effectiveness coefficient**  $\Gamma$ , which quantifies the expected increment in real reward per unit increment in virtual reward. We model it as the product of three key factors:

- $C_{\text{tool}}$ : Tool capability determines the probability of logical execution being reproduced in reality.
- $\Phi_{\text{plan}}$ : Plan sufficiency determines the strength of association between correct logic and high-quality output.
- $\kappa(\pi_{\text{pst}})$ : Anchoring strength of the PST prior, indicating the degree to which the policy remains in a “reasonable” distribution region during VRL optimization, with  $\kappa \in (0, 1]$ . Strong anchoring ( $\kappa \approx 1$ ) ensures the optimization direction remains effective in the real world.

Therefore, we assume a monotonic relationship:

$$J_{\text{real}}(\pi_{\text{VRL}}) - J_{\text{real}}(\pi_{\text{pst}}) \geq \Gamma \cdot \Delta R_{\text{vrt}} - \mathcal{E}(\pi_{\text{VRL}}), \quad \text{where } \Gamma = C_{\text{tool}} \cdot \Phi_{\text{plan}} \cdot \kappa(\pi_{\text{pst}}). \quad (2)$$

When  $\Gamma > 0$ , the logical improvement brought by virtual optimization can be partially translated into real-world improvement.

**Step 3.3: Derive the Final Lower Bound** Substituting  $\Delta R_{\text{vrt}} = \mathbb{E}_{\pi}[\Delta R_{\text{vrt}}]$  into inequality (2) yields the lower bound stated in Theorems 4.2:

$$J_{\text{real}}(\pi_{\text{VRL}}) - J_{\text{real}}(\pi_{\text{pst}}) \geq \Gamma \cdot \mathbb{E}_{\pi}[\Delta R_{\text{vrt}}] - \mathcal{E}(\pi_{\text{VRL}}).$$

**Step 3.4: Condition for Non-Negative Improvement** From the inequality in Theorems 4.2, the **sufficient condition** for non-negative improvement in real-world performance (i.e.,  $J_{\text{real}}(\pi_{\text{VRL}}) \geq J_{\text{real}}(\pi_{\text{pst}})$ ) is directly obtained as:

$$\Gamma \cdot \mathbb{E}_{\pi}[\Delta R_{\text{vrt}}] \geq \mathcal{E}(\pi_{\text{VRL}}).$$

This means that the **Causal Improvement** brought by virtual training must be sufficient to cover the **Transfer Loss** arising from simulation imperfections. This does not require  $C_{\text{tool}} = 1$  or  $\Phi_{\text{plan}} = 1$ ; as long as their product combined with the anchoring strength is large enough to make  $\Gamma$  sufficiently large, and VRL can effectively increase  $\Delta R_{\text{vrt}}$  (as shown in experiments where virtual reward exceeds 95%), positive transfer is guaranteed. ■

## Summary

Through formal modeling, this derivation decomposes the challenge of sim-to-real transfer into differences at the dynamic, reward, and policy levels, and quantifies their upper bounds using key variables such as tool capability, plan sufficiency, and PST prior. Theorems 4.1 shows that systematic error can be controlled by improving tool fidelity, strengthening PST anchoring, and optimizing plan-result alignment. Theorems 4.2 further proves that as long as virtual training can effectively enhance the agent’s logical capabilities (Causal Improvement) and this improvement outweighs the bounded systematic error (Transfer Loss), performance improvement in the real world is guaranteed. This provides a solid theoretical foundation for the application of virtual reinforcement learning in high-dimensional, long-horizon tasks such as visual creation.

Table 5: Human Evaluation of Detailed Dimensions on VisGenBench-Image (Score = Success Rate  $\times$  Human Evaluation Score)

Model	Semantic Matching	Style Matching	Emotion Matching	Subject Consistency	Design Integrity	Visual Integrity	Text Quality	Creativity	Overall
GPT-5	3.4883	3.6214	2.9656	3.6024	3.4408	3.4218	2.7565	3.4408	3.3458
Gemini2.5-Pro	3.3943	3.5399	2.8119	3.4034	3.2214	3.2669	2.7300	3.3215	<b>3.2123</b>
Qwen3-VL-32B-Tk	3.4435	3.7248	2.9876	3.5890	3.4047	3.4823	2.8130	3.4726	3.3659
Qwen3-VL-32B-SFT	3.3504	3.8016	2.8896	3.7632	3.4368	3.5040	2.8224	3.5232	<b>3.3888</b>
VisionCreator-32B	3.6432	3.8412	3.1581	3.7620	3.4452	3.6531	2.8809	3.5739	<b>3.4947</b>

Table 6: Human Evaluation of Detailed Dimensions on VisGenBench-Video (Score = Success Rate  $\times$  Human Evaluation Score)

Model	Script	Story-board	Content Consistency	Subject Consistency	Video Effect	Visual Motion	
GPT-5	3.1062	2.9202	3.1434	3.1713	3.0597	3.0039	
Gemini2.5-Pro	2.9484	2.6796	3.0156	2.856	2.8728	2.6628	
Qwen3-VL-32B-Thinking	3.069	2.9016	3.1713	3.162	2.9574	2.9388	
Qwen3-VL-32B-SFT	3.6002	2.867	3.5814	3.3652	3.243	2.9328	
VisionCreator-32B	3.5616	3.1872	3.5808	3.4176	3.4752	3.2256	

Model	Audio-Visual	Music	Dubbing	Subtitle	Transition	Editing	Overall
GPT-5	3.0411	3.2643	2.8644	2.9788	2.8812	2.8392	2.814
Gemini2.5-Pro	2.8056	2.7888	2.8728	2.8812	2.8392	2.562	2.814
Qwen3-VL-32B-Thinking	2.9481	2.9202	3.1341	3.069	2.9295	2.8737	3.0039
Qwen3-VL-32B-SFT	3.1772	3.0644	3.2148	3.0174	3.0268	2.9328	3.1678
VisionCreator-32B	3.3792	3.2928	3.3888	3.3216	3.2352	3.1104	<b>3.3504</b>

Table 7: General-purpose Datasets.

Category	Name	Quantity
NLP	DeepSeek-R1-Distill-110k Liu (2025)	110k
	LONGCOT-Refine-500K PowerInfer Team (2025)	500k
	alpaca-gpt4-data Peng et al. (2023a,b)	100k
Multimodal	M3IT Li et al. (2023)	1592k
Tool Calling	function-calling-chatml Glaive AI (2023)	112k
	xlam-function-calling-60k Zhang et al. (2024)	60k
	ms-agent ModelScope Team (2024)	600k
	ToolACE Liu et al. (2025)	11k
	ToolBench Qin et al. (2024)	123k
	AFM Li et al. (2025b)	76k

Table 8: Task Distribution in VisGenData-4k Dataset

Video Generation Tasks		Image Generation Tasks	
No.	Task Type	No.	Task Type
1.	Product marketing videos	1.	Product images
2.	Public service advertisements	2.	Detail pages
3.	Corporate promotion videos	3.	Key Visual (KV)
4.	Brand story videos	4.	Landing pages / H5 graphics
5.	Event promotion videos	5.	Complete brand visual identity
6.	Instructional videos	6.	Banner graphics
7.	Popular science documentaries	7.	Official account cover images
8.	Music videos (MV)	8.	Xiaohongshu covers
9.	Concert recordings	9.	Marketing posters
10.	Variety shows	10.	Avatar design
11.	Story videos	11.	Static emoji generation
12.	Video podcasts	12.	ICON design
13.	Picture books	13.	LOGO design
14.	Dynamic comics	14.	Mini-game UI design
15.	Animated short films	15.	Character design
16.	Animated movies	16.	Character action design
17.	Game adaptation films	17.	Scene design
18.	Game videos	18.	Storyboards
19.	Movies	19.	Picture Book
20.	Short dramas	20.	Stylization
21.	Story explanations	21.	Realistic Photography

Table 9: VisGenEnv integrates 36 visual creation tools.

Tool Category	Tool Function	Tool Name
Text-to-Text	Storyboard Text Polishing (Claude)	tool_prompt_refine
	Storyboard Generation (Claude)	tool_video_shot_gen
	Script Tool (Claude)	tool_video_script_gen
	Storyboard Polishing (Claude)	tool_storyboard_polish
	Script & Storyboard Polishing	tool_script_storyboard_merge
Text-to-Image	Text-to-Video (Veo3)	tool_text2video_veo
	Text-to-Image (nano-banana)	tool_text2image_gemini
	Text-to-Image (hunyuan)	tool_text2image_hunyuan
	Text-to-Image (ByteDance)	tool_text2image_seed
	Text-to-Image (GPT)	tool_text2image_gpt
Image-to-Image	Text-to-Image (Qwen)	tool_text2image_qwen
	Image-to-Image (nano-banana)	tool_image_edit_gemini
	Image-to-Image (Qwen)	tool_image_edit_qwen
Image-to-Video	Image-to-Image (GPT)	tool_image_edit_gpt
	Image-to-Video (Keling)	tool_image2video_keling
Audio Generation	Image-to-Video (Veo3)	tool_image2video_veo3
	Music Generation (Suno)	tool_music_suno
	Video Sound Effect Generation	tool_sound_fx_gen
	TTS Generation	tool_tts_generation
	Video Composition (MoviePy)	tool_video_composite
	Video Clip - MoviePy Post-processing	tool_video_postprocess
	Video Generation Automation Pipeline	tool_video_auto_pipeline
	Beat Detection Tool	tool_beat_detect
	Video Editing (Trim)	tool_video_trim_edit
	Video Speed Change	tool_video_speed_adjust
	TTS + Composition Tool	tool_tts_composite
	Audio Editing	tool_audio_edit_cut
Multimodal Understanding	Add Subtitles	tool_subtitle_add_text
	Video Understanding (Gemini2.5-Pro)	tool_video_analysis
	Audio Understanding (Gemini2.5-Pro)	tool_audio_analysis
Other	Image Understanding (Gemini2.5-Pro)	tool_image_analysis
	Tavily Search - Content Extraction	tool_search_content
	Inspiration Search	tool_search_inspire
	Summary Tool	tool_content_summary
	To-Do List	tool_task_manager
	HTML Generation Tool	tool_html_builder

**Query:** Produce a product marketing video consisting of 8 scenes, set in a modern home living room with morning sunlight streaming through floor-to-ceiling windows. The video should vividly showcase the smart speaker's usage scenarios at different times of the day:

- (1) Morning news briefing with sunlight casting changing shadows on the speaker
- (2) Noon music playback, framed harmoniously with indoor plants
- (3) Afternoon voice-controlled smart home operation, capturing the dynamic movement of curtains opening and closing
- (4) Evening ambiance creation, highlighting the interplay between the speaker's lighting and the sunset glow
- (5) Nighttime home theater mode, demonstrating its projection effects
- (6) Night mode for sleep assistance, showcasing the soft glow in the environment
- (7) Weekend party scenario with multi-room audio synchronization
- (8) Rainy day cozy home atmosphere, blending seamlessly with the interior warmth

Each scene must maintain the same living room layout and furniture arrangement.

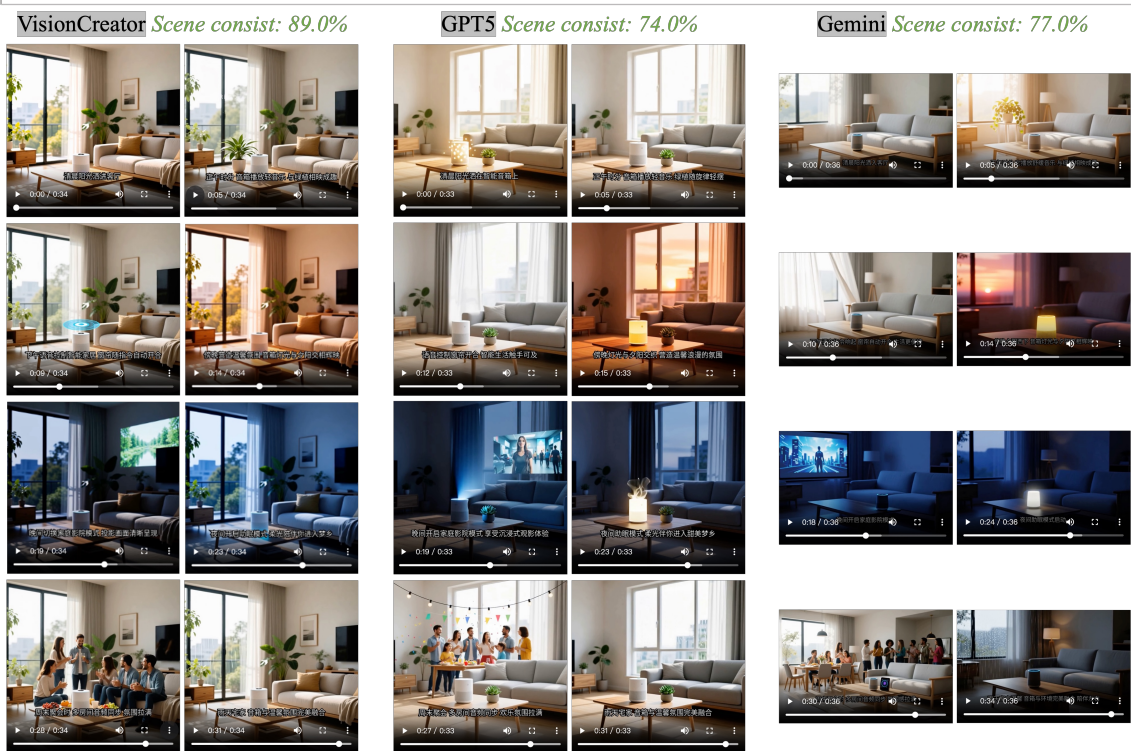


Figure 10: Visualizations for scene consistency.

**Query:** Generate 10 character illustrations of the game character "Elf Archer" with green short hair, pointed ears, and wielding a long bow. Include the following different skins: Primeval Forest, Ice Queen, Desert Traveler, Night Assassin, Flower Fairy, Ocean Melody, Starry Fantasy, Holiday Limited, Battle Gear, and Casual Wear.

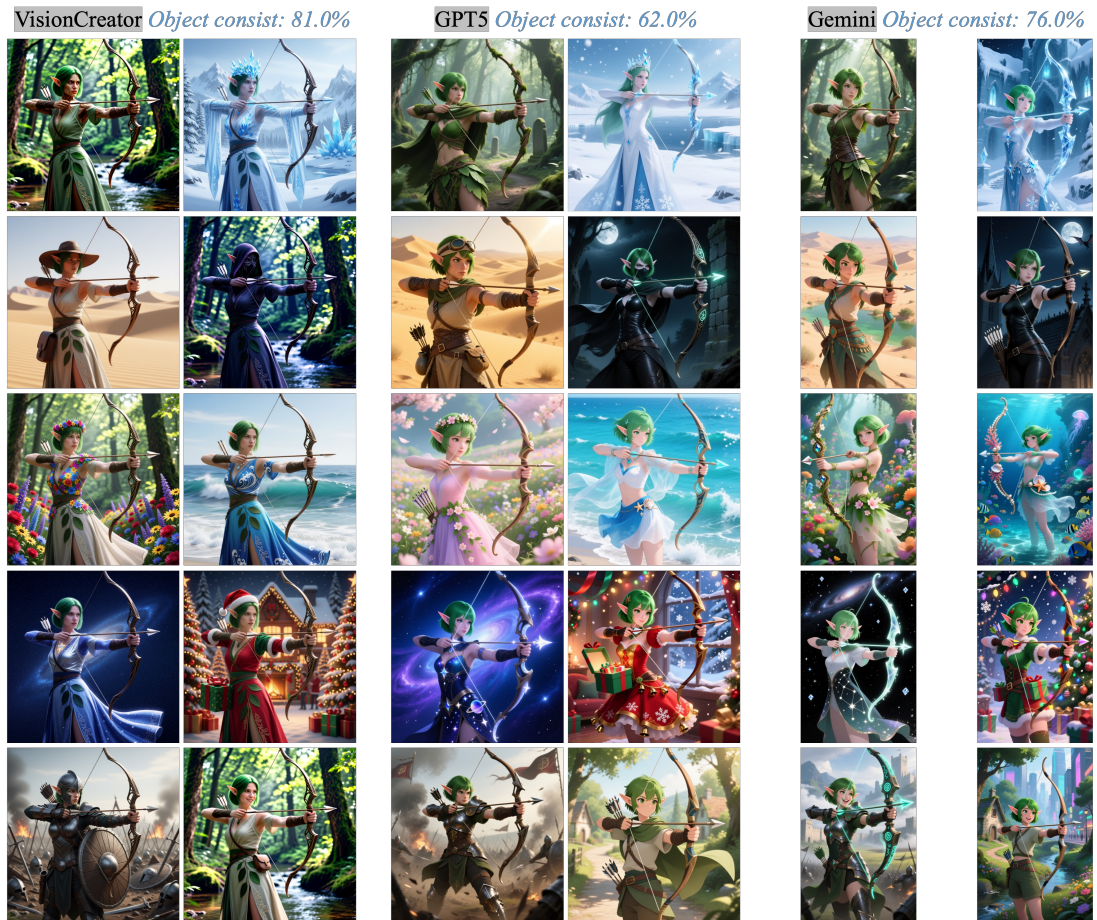


Figure 11: Visualizations for object consistency.

**画面1: 特写镜头。**一个由彩色毛毡和绒线制成的奇幻小屋窗口,一只好奇的毛毡小狐狸(或小朋友)探出头来,眼睛闪闪发光。配音:“咦?是什么地方,这么香甜甜甜?”画面1:镜头拉远,全景展示毛毡风格的“芬达汽水工坊”。小屋由各种水果形状的毛毡块拼接而成,屋顶是巨大的橙色切片,烟囱冒着气泡状的毛毡云朵。配音:“欢迎来到芬达奇幻工厂!这里的一切,都好Q弹!”画面3:室内中景。毛毡小狐狸看到几个穿着围裙的毛毡卡通“可乐瓶”正在忙碌,它们将一个个真实的、毛茸茸的橙子投入冒着七彩气泡的魔法大锅。配音:“看,他们把阳光橙子变成魔法啦!”画面4:创意夸张。魔法锅中的橙色液体被倒入一个毛毡编织的管道。管道像滑梯一样,液体流过时,周围跳出许多毛毡小球欢呼雀跃,表现气泡的欢腾。配音:“每一个泡泡,都是快乐的精灵在跳舞!”画面5:镜头切换至一片由橙色毛毡编织的“芬达海”,海浪是绵密的泡沫。一艘小汽水船帆船在海面航行。配音:“不可思议吧?这里就是快乐的芬达海!”画面6:近景。毛毡小狐狸和它的毛毡小动物朋友们(小熊、小兔)每人捧着一杯冒着气泡的芬达,互相干杯,脸上露出满足的笑容,身体随着音乐轻轻摇摆。配音:“和好朋友一起,快乐才会冒泡泡呀!”画面7:动态定格动画。一瓶真实的芬达饮料被毛毡制作的花朵和水果环绕,瓶身上凝结着毛毡小水珠,凸显冰凉感。配音:“芬达,你的快乐气泡水!”画面8:全景。所有毛毡角色和小屋融化成芬达的Logo,Logo也是由毛毡勾勒而成,温暖可爱。屏幕上出现广告语。配音:“芬达奇幻之旅,等你来开启!”

**生成结果**

素材文件

全部 图片 视频 音频

**需求分析**

我先分析当前情况。

用户已经提供了一套完整的分镜脚本描述,包含了8个画面的场景、角色、动作、配音等详细信息。根据历史任务上下文,我之前已经输出了初始待办列表,并且任务处于“理解需求并制定计划”阶段。结合可用工具列表和任务需求,这明显是一个剧情类视频生成任务,涉及多个分镜画面,需要先生成参考图保证主体一致性,再生成关键帧,最后生成视频片段。

由于用户提供了完整的分镜脚本,我无需再调用脚本工具生成脚本,可以直接进入执行阶段。在初始待办列表中,已经有“生成主角参考图”和“生成第1个关键帧”等步骤,但没有明确列出每个分镜对应的图片生成和视频生成任务。

因此,我需要在plan中补充完整:

1. 生成主角参考图(毛毡小狐狸,毛毡小动物朋友们,可乐瓶角色,芬达汽水工坊主体)
2. 生成8个分镜关键帧(基于每个分镜的image\_prompt)
3. 生成8个分镜视频片段(基于关键帧和分镜视频prompt)
4. 合成最终视频(如果有配音和背景音乐)

关于BGM和配音:

- 用户未明确要求,但脚本中有背景音乐描述(“芬达奇幻工厂”背景音乐、节奏感等),根据规则必须检查脚本并强制添加背景音乐。
- 脚本中每个分镜都有配音文案,因此必须添加TTS配音。
- 鼓点检测不适用,因为这是普通剧情视频,非节奏感强或MV。

所以我在plan中需要补充背景音乐生成和TTS配音任务。

综上,我将输出初始待办列表,包含所有必要步骤,并明确调用的工具类型。

**任务规划**

1. 目标:生成毛毡小狐狸等主要角色参考图,确保后续所有分镜中主体外观一致。工具:图生图(consistency模式),使用生成的图片作为参考图。
2. 目标:基于每个分镜的image\_prompt生成静态关键帧图像。工具:文生图(每个分镜单独调用一次)。
3. 目标:基于每个分镜的关键帧图像和video\_prompt生成动态视频片段。工具:生视频(每个分镜单独调用一次)。
4. 目标:为每个视频片段添加TTS配音。工具:给视频添加TTS和字幕(每个视频片段分别调用)。
5. 目标:生成背景音乐(BGM)。工具:音乐生成(基于脚本中的bgm描述)。
6. 目标:将所有视频片段和背景音乐合成最终视频。工具:视频合成。

**任务执行**

我先分析当前情况。

用户的分镜脚本已经完整提供,包含8个分镜的详细描述,因此我无需再调用脚本工具生成脚本。任务已经进入执行阶段。初始待办列表中已经有6个步骤,分别是生成角色参考图、关键帧、视频片段、TTS配音、背景音乐和视频合成。

根据规则,对于需要保持主体一致性的任务,必须先为每个需要保持一致的主体生成参考图。本任务的主体包括:毛毡小狐狸、毛毡小动物朋友们(小熊、小兔)、可乐瓶角色、芬达汽水工坊主体。这些主体需要在后续的关键帧生成中保持一致,因此第一步是生成这些角色的参考图。

下一步应执行任务1:生成毛毡小狐狸等主要角色参考图。由于用户没有提供参考图URL,我需要使用文生图工具,为每个角色生成一个清晰的参考图,描述要详细,包括面部、体型、服装、发型等关键特征。生成参考图后,后续步骤才能基于这些参考图进行关键帧生成(使用图生图的consistency模式)。

因此,当前阶段应该调用文生图工具为每个角色生成参考图。

任务执行

任务执行

任务执行

任务执行

**任务执行**

我先分析当前情况。

上一轮已经成功调用视频合成将所有配音视频片段和背景音乐合成最终视频(<https://multimodel-agent-1258344703.cos.accelerate.myqcloud.com/upload/vision-tool/e008ecc0-dcf6-47d7-98bc-c4655a6cbef0/9dca40d-996f-4987-96c3-ceb7f99ed752.mp4>)。根据初始待办列表,任务6的目标是将所有视频片段和背景音乐合成最终视频,现在已成功完成。

检查待办列表:

- 任务1(生成参考图):已完成
- 任务2(生成关键帧):已完成
- 任务3(生成视频片段):已完成
- 任务4(TTS配音):已完成
- 任务5(生成背景音乐):已完成
- 任务6(视频合成):已完成

所有任务步骤都已完成,目标视频<https://multimodel-agent-1258344703.cos.accelerate.myqcloud.com/upload/vision-tool/e008ecc0-dcf6-47d7-98bc-c4655a6cbef0/9dca40d-996f-4987-96c3-ceb7f99ed752.mp4>已经生成,可以交付给用户。

因此任务已经完成,可以进入总结并输出最终结果。

**执行结果**

```
{
  "task_status": "success",
  "answer_url_list": [
    "https://multimodel-agent-1258344703.cos.accelerate.myqcloud.com/upload/vision-tool/e008ecc0-dcf6-47d7-98bc-c4655a6cbef0/9dca40d-996f-4987-96c3-ceb7f99ed752.mp4"
  ],
  "summary": "已成功生成所需的视觉内容。首先生成了毛毡小狐狸、毛毡小熊、毛毡小兔、可乐瓶角色和芬达汽水工坊的参考图,确保主体一致性。随后基于参考图生成了8个分镜的关键帧图像,并使用这些关键帧生成了动态视频片段。接着为每个视频片段添加了TTS配音,并生成了温馨可爱的背景音乐。最后将所有视频片段与背景音乐合成,得到最终的芬达奇幻工厂动画视频。视频内容完整,符合脚本描述,风格温馨可爱,色彩明亮,节奏感强。"
}
```

Figure 12: Demo page.

---

## References

- Andreas Blattmann, Tim Dockhorn, Sumith Kulal, Daniel Mendelevitch, Maciej Kilian, Dominik Lorenz, Yam Levi, Zion English, Vikram Voleti, Adam Letts, et al. Stable video diffusion: Scaling latent video diffusion models to large datasets. *arXiv preprint arXiv:2311.15127*, 2023.
- Mark Chen, Alec Radford, Rewon Child, Jeffrey Wu, Heewoo Jun, David Luan, and Ilya Sutskever. Generative pretraining from pixels. In *International conference on machine learning*, pp. 1691–1703. PMLR, 2020.
- comfyanonymous. Comfyui. <https://github.com/comfyanonymous/ComfyUI>, 2023. GitHub repository.
- Yufeng Cui, Honghao Chen, Haoge Deng, Xu Huang, Xinghang Li, Jirong Liu, Yang Liu, Zhuoyan Luo, Jinsheng Wang, Wenxuan Wang, et al. Emu3. 5: Native multimodal models are world learners. *arXiv preprint arXiv:2510.26583*, 2025.
- Chaorui Deng, Deyao Zhu, Kunchang Li, Chenhui Gou, Feng Li, Zeyu Wang, Shu Zhong, Weihao Yu, Xiaonan Nie, Ziang Song, et al. Emerging properties in unified multimodal pretraining. *arXiv preprint arXiv:2505.14683*, 2025.
- Patrick Esser, Sumith Kulal, Andreas Blattmann, Rahim Entezari, Jonas Müller, Harry Saini, Yam Levi, Dominik Lorenz, Axel Sauer, Frederic Boesel, et al. Scaling rectified flow transformers for high-resolution image synthesis. In *Forty-first International Conference on Machine Learning*, 2024.
- Lijie Fan, Tianhong Li, Siyang Qin, Yuanzhen Li, Chen Sun, Michael Rubinstein, Deqing Sun, Kaiming He, and Yonglong Tian. Fluid: Scaling autoregressive text-to-image generative models with continuous tokens. *arXiv preprint arXiv:2410.13863*, 2024.
- Glaive AI. Function-calling-chatml: Function calling dataset in chatml format. <https://modelscope.cn/datasets/AI-ModelScope/function-calling-chatml>, 2023.
- Litao Guo, Xinli Xu, Luozhou Wang, Jiantao Lin, Jinsong Zhou, Zixin Zhang, Bolan Su, and Ying-Cong Chen. Comfymind: Toward general-purpose generation via tree-based planning and reactive feedback. *arXiv preprint arXiv:2505.17908*, 2025.
- Jian Han, Jinlai Liu, Yi Jiang, Bin Yan, Yuqi Zhang, Zehuan Yuan, Bingyue Peng, and Xiaobing Liu. Infinity: Scaling bitwise autoregressive modeling for high-resolution image synthesis. *arXiv preprint arXiv:2412.04431*, 2024.
- Jonathan Ho, Ajay Jain, and Pieter Abbeel. Denoising diffusion probabilistic models. *Advances in neural information processing systems*, 33:6840–6851, 2020.
- Oucheng Huang, Yuhang Ma, Zeng Zhao, Mingrui Wu, Jiayi Ji, Rongsheng Zhang, Zhipeng Hu, Xiaoshuai Sun, and Rongrong Ji. Comfygpt: A self-optimizing multi-agent system for comprehensive comfyui workflow generation. *arXiv preprint arXiv:2503.17671*, 2025.
- Black Forest Labs. Flux. <https://github.com/black-forest-labs/flux>, 2024.
- Jinxiang Lai, Jie Zhang, Jun Liu, Jian Li, Xiaocheng Lu, and Song Guo. Spider: Any-to-many multimodal llm. *arXiv preprint arXiv:2411.09439*, 2024.
- Lei Li, Yuwei Yin, Shicheng Li, Liang Chen, Peiyi Wang, Shuhuai Ren, Mukai Li, Yazheng Yang, Jingjing Xu, Xu Sun, Lingpeng Kong, and Qi Liu. M<sup>3</sup>it: A large-scale dataset towards multimodal multilingual instruction tuning. In *arXiv preprint arXiv:2306.04387*, June 2023. URL <https://arxiv.org/abs/2306.04387>.
- Shufan Li, Konstantinos Kallidromitis, Akash Gokul, Zichun Liao, Yusuke Kato, Kazuki Kozuka, and Aditya Grover. Omniflow: Any-to-any generation with multi-modal rectified flows. In *Proceedings of the Computer Vision and Pattern Recognition Conference*, pp. 13178–13188, 2025a.

- 
- Weizhen Li, Jianbo Lin, Zhuosong Jiang, Jingyi Cao, Xinpeng Liu, Jiayu Zhang, Zhenqiang Huang, Qianben Chen, Weichen Sun, Qiexiang Wang, Hongxuan Lu, Tianrui Qin, Chenghao Zhu, Yi Yao, Shuying Fan, Xiaowan Li, Tiannan Wang, Pai Liu, King Zhu, He Zhu, Dingfeng Shi, Piaohong Wang, Yeyi Guan, Xiangru Tang, Minghao Liu, Yuchen Eleanor Jiang, Jian Yang, Jiaheng Liu, Ge Zhang, and Wangchunshu Zhou. Chain-of-agents: End-to-end agent foundation models via multi-agent distillation and agentic rl. arXiv preprint arXiv:2508.13167, August 2025b. URL <https://arxiv.org/abs/2508.13167>.
- Bin Lin, Yunyang Ge, Xinhua Cheng, Zongjian Li, Bin Zhu, Shaodong Wang, Xianyi He, Yang Ye, Shenghai Yuan, Liuhan Chen, et al. Open-sora plan: Open-source large video generation model. arXiv preprint arXiv:2412.00131, 2024.
- Cong Liu. Chinese-deepseek-r1-distill-data-110k-sft. <https://modelscope.cn/datasets/liucong/Chinese-DeepSeek-R1-Distill-data-110k-SFT>, 2025.
- Weiwen Liu, Xu Huang, Xingshan Zeng, Xinlong Hao, Shuai Yu, Dexun Li, Shuai Wang, Weinan Gan, Zhengying Liu, Yuanqing Yu, Zezhong Wang, Yuxian Wang, Wu Ning, Yutai Hou, Bin Wang, Chuhan Wu, Xinzhi Wang, Yong Liu, Yasheng Wang, Duyu Tang, Dandan Tu, Lifeng Shang, Xin Jiang, Ruiming Tang, Defu Lian, Qun Liu, and Enhong Chen. Toolace: Winning the points of llm function calling. In International Conference on Learning Representations (ICLR), 2025. URL <https://arxiv.org/abs/2409.00920>.
- ModelScope Team. Ms-agent: Modelscope agent sft dataset. [https://modelscope.cn/datasets/ic/ms\\_agent](https://modelscope.cn/datasets/ic/ms_agent), 2024.
- Yatian Pang, Peng Jin, Shuo Yang, Bin Lin, Bin Zhu, Zhenyu Tang, Liuhan Chen, Francis EH Tay, Ser-Nam Lim, Harry Yang, et al. Next patch prediction for autoregressive visual generation. arXiv preprint arXiv:2412.15321, 2024.
- William Peebles and Saining Xie. Scalable diffusion models with transformers. In Proceedings of the IEEE/CVF International Conference on Computer Vision, pp. 4195–4205, 2023.
- Baolin Peng, Chunyuan Li, Pengcheng He, Michel Galley, and Jianfeng Gao. Alpaca-gpt4-data-en: English instruction following dataset. <https://modelscope.cn/datasets/AI-ModelScope/alpaca-gpt4-data-en>, 2023a.
- Baolin Peng, Chunyuan Li, Pengcheng He, Michel Galley, and Jianfeng Gao. Alpaca-gpt4-data-zh: Chinese instruction following dataset. <https://modelscope.cn/datasets/AI-ModelScope/alpaca-gpt4-data-zh>, 2023b.
- PowerInfer Team. Longcot-refine-500k: Long chain-of-thought reasoning dataset. <https://modelscope.cn/datasets/PowerInfer/LONGCOT-Refine-500K>, 2025.
- Yujia Qin, Shihao Liang, Yining Ye, Kunlun Zhu, Lan Yan, Yaxi Lu, Yankai Lin, Xin Cong, Xiangru Tang, Bill Qian, Sihan Zhao, Lauren Hong, Runchu Tian, Ruobing Xie, Jie Zhou, Mark Gerstein, Dahai Li, Zhiyuan Liu, and Maosong Sun. Toolllm: Facilitating large language models to master 16000+ real-world apis. In International Conference on Learning Representations (ICLR), 2024. URL <https://arxiv.org/abs/2307.16789>.
- Aditya Ramesh, Prafulla Dhariwal, Alex Nichol, Casey Chu, and Mark Chen. Hierarchical text-conditional image generation with clip latents. arXiv preprint arXiv:2204.06125, 1(2):3, 2022.
- Chitwan Saharia, William Chan, Saurabh Saxena, Lala Li, Jay Whang, Emily L Denton, Kamyar Ghasemipour, Raphael Gontijo Lopes, Burcu Karagol Ayan, Tim Salimans, et al. Photorealistic text-to-image diffusion models with deep language understanding. Advances in neural information processing systems, 35:36479–36494, 2022.
- Uriel Singer, Adam Polyak, Thomas Hayes, Xi Yin, Jie An, Songyang Zhang, Qiyuan Hu, Harry Yang, Oron Ashual, Oran Gafni, et al. Make-a-video: Text-to-video generation without text-video data. arXiv preprint arXiv:2209.14792, 2022.
- Peize Sun, Yi Jiang, Shoufa Chen, Shilong Zhang, Bingyue Peng, Ping Luo, and Zehuan Yuan. Autoregressive model beats diffusion: Llama for scalable image generation. arXiv preprint arXiv:2406.06525, 2024.

- 
- Keyu Tian, Yi Jiang, Zehuan Yuan, Bingyue Peng, and Liwei Wang. Visual autoregressive modeling: Scalable image generation via next-scale prediction. [arXiv preprint arXiv:2404.02905](#), 2024.
- Weijia Wu, Zeyu Zhu, and Mike Zheng Shou. Automated movie generation via multi-agent cot planning. [arXiv preprint arXiv:2503.07314](#), 2025.
- Junfei Xiao, Ceyuan Yang, Lvmin Zhang, Shengqu Cai, Yang Zhao, Yuwei Guo, Gordon Wetzstein, Maneesh Agrawala, Alan Yuille, and Lu Jiang. Captain cinema: Towards short movie generation. [arXiv preprint arXiv:2507.18634](#), 2025.
- Xuenan Xu, Jiahao Mei, Chenliang Li, Yuning Wu, Ming Yan, Shaopeng Lai, Ji Zhang, and Mengyue Wu. Mm-storyagent: Immersive narrated storybook video generation with a multi-agent paradigm across text, image and audio. [arXiv preprint arXiv:2503.05242](#), 2025a.
- Zhenran Xu, Yiyu Wang, Xue Yang, Longyue Wang, Weihua Luo, Kaifu Zhang, Baotian Hu, and Min Zhang. Comfyui-r1: Exploring reasoning models for workflow generation. [arXiv preprint arXiv:2506.09790](#), 2025b.
- Xiangyuan Xue, Zeyu Lu, Di Huang, Zidong Wang, Wanli Ouyang, and Lei Bai. Comfybench: Benchmarking llm-based agents in comfyui for autonomously designing collaborative ai systems. In *Proceedings of the Computer Vision and Pattern Recognition Conference*, pp. 24614–24624, 2025.
- Zhuoyi Yang, Jiayan Teng, Wendi Zheng, Ming Ding, Shiyu Huang, Jiazheng Xu, Yuanming Yang, Wenyi Hong, Xiaohan Zhang, Guanyu Feng, et al. Cogvideox: Text-to-video diffusion models with an expert transformer. [arXiv preprint arXiv:2408.06072](#), 2024.
- Jianguo Zhang, Tian Lan, Ming Zhu, Zuxin Liu, Thai Hoang, Shirley Kokane, Weiran Yao, Juntao Tan, Akshara Prabhakar, Haolin Chen, Zhiwei Liu, Yihao Feng, Tulika Awalgaoonkar, Rithesh Murthy, Eric Hu, Zeyuan Chen, Ran Xu, Juan Carlos Niebles, Shelby Heinecke, Huan Wang, Silvio Savarese, and Caiming Xiong. xlam: A family of large action models to empower ai agent systems. [arXiv preprint arXiv:2409.03215](#), September 2024. URL <https://arxiv.org/abs/2409.03215>.
- Dian Zheng, Ziqi Huang, Hongbo Liu, Kai Zou, Yinan He, Fan Zhang, Lulu Gu, Yuanhan Zhang, Jingwen He, Wei-Shi Zheng, et al. Vbench-2.0: Advancing video generation benchmark suite for intrinsic faithfulness. [arXiv preprint arXiv:2503.21755](#), 2025.